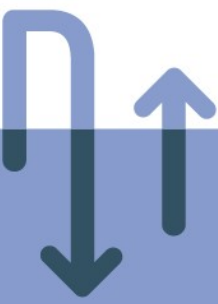


scan 



Fracture characterization of the Dinantian carbonates in the Dutch Subsurface

Report by SCAN

November 2019

This page intentionally left blank

Fracture characterization of the Dinantian carbonates in the Dutch subsurface

Written by:

Douwe van Leverink¹ & Kees Geel²

FMI evaluation by:

Panterra Geoconsultants B.V.

November 2019

1- Energie Beheer Nederland (EBN), Daalsesingel 1, 3511 SV Utrecht, The Netherlands

2- Geological Survey of the Netherlands (TNO), Princetonlaan 6, 3584 CB Utrecht, the Netherlands

Dit rapport is een product van het SCAN-programma en wordt mogelijk gemaakt door het Ministerie van Economische Zaken en Klimaat

Contents

1	Samenvatting (Dutch).....	6
2	Executive summary	8
3	Introduction.....	9
3.1	Importance of fractures for Dinantian	9
3.2	This report	10
4	Fractures.....	11
4.1	Fractured carbonate reservoirs.....	12
4.1.1	Flow enhancement of carbonate reservoir.....	13
4.2	Fracture aperture	14
4.2.1	Factors that influence fracture apertures	16
4.2.2	Data on fracture apertures.....	18
4.2.3	Summary.....	20
4.3	Fracture density.....	22
5	Fracture characterization components and implications	24
5.1	Seismic interpretation	24
5.2	Tectonic evolution	25
5.3	Present day stress field	25
5.4	Rock mechanical properties	25
5.5	Flow estimation	26
5.6	Development considerations	26
5.7	Well type	28
6	Dinantian fracture observations.....	29
6.1	Observations from Dinantian outcrops and analogues.....	29
6.2	Fracture observations from seismic.....	29
6.3	Fracture observations from well data	30
6.3.1	Dinantian drilling events.....	30
6.3.2	Dinantian cores.....	30
6.3.3	Log observations Dinantian	33
6.3.4	Well test observations Dinantian wells	33
7	FMI interpretation Dinantian wells	35
7.1	FMI Belgian wells.....	35
7.2	FMI LTG-01 & CAL-GT-01.....	35
7.2.1	FMI evaluation LTG-01	35
7.2.2	FMI evaluation CAL-GT-01	44

7.2.3	Discussion FMI interpretations.....	51
7.3	Conclusions FMI.....	52
8	Conclusions.....	53
9	Recommendations.....	54
10	Acknowledgements	55
11	References.....	56
12	Appendix A: Data table well data.....	61
13	Appendix B: Table with fracture indications from drilling, logs, core recovery and well tests.	62
14	Appendix C: Table of data files shared via www.nlog.nl/scan	71

1 Samenvatting (Dutch)

Dinantien kalksteen is overwegend niet permeabel, waardoor productie van water uit deze reservoirs geaccommodeerd worden door *fractures* (scheuren) en / of karst. Hoofdvragen voor geothermische ontwikkeling zijn; bestaan er open fractuursystemen, hoe zijn deze lateraal en verticaal verdeeld, vormen ze een uitgebreid netwerk om consistent voldoende volumes te produceren en - indien aanwezig - hoe zijn ze georiënteerd. Het karakteriseren van *fractures* (bijv. oriëntatie, grootte, breedte, frequentie) is daarom een belangrijke stap in de richting van geothermische exploratie en ontwikkeling van de Dinantien kalksteen.

Fracture kenmerken worden beïnvloed door verschillende factoren, zoals geologische en hydrologische geschiedenis, historische en huidige spanning uitgeoefend op het gesteente, maar mogelijk ook door laagdikte, facies, lithologie. Het vinden van een verband tussen *fracture* kenmerken en de bovenstaande factoren vereist inzicht in de timing in de geologische geschiedenis waarbij elke afzonderlijke factor veranderde en hoe dit de breuken heeft beïnvloed. Dit kan worden afgeleid van een combinatie van verschillende gegevenstypen zoals; hoge resolutie 3D seismische gegevens, putgegevens en productiegegevens. Zelfs voor reservoirs met aanzienlijke hoeveelheden gegevens van hoge kwaliteit kan het begrijpen van reservoirproductiviteit en productiviteitsvoorspelling echter extreem uitdagend zijn. Gezien dit gegeven, wordt de *fracture* karakterisering van Dinantien carbonaten in Nederland ernstig belemmerd door de beperkte hoeveelheid gegevens. Daarom zullen toekomstige activiteiten over dit onderwerp sterk afhankelijk zijn van scenario's met een breed scala aan *fracture* kenmerken, die vaak gebaseerd zullen zijn op een beperkte hoeveelheid lokale gegevens en veel analogen. De beperkingen die aan het gebruik daarvan kleven worden in dit rapport ook beschreven. In nieuwe boringen naar Dinantien carbonaten zou een uitgebreid data-acquisitie programma moeten plaatsvinden over de Dinantien sectie, met daarin bij voorbeeld *borehole imaging, acoustic logs en kernen*.

Dit rapport biedt een start voor de karakterisering van Dinantien *fractures*. Het vat algemene informatie over *fractures* samen, het bespreekt *de* activiteiten die bij dit soort beoordelingen kunnen worden uitgevoerd, maar die niet allemaal in deze studie zijn gedaan vnl. vanwege het gebrek aan data. Hierbij wordt o.a. verwezen naar andere SCAN-rapporten. Bovendien verwijst het rapport naar enkele gegevens van analogen waarop in de nabije toekomst verder kan worden gebouwd. Waarnemingen die (mogelijk) duiden op *fractures* in Nederlandse putten die de Dinantien hebben aangeboord, zijn samengevat uit meerdere bronnen. Voor dit rapport werden de FMI boorgatmetingen – van de LTG-01 en CAL-GT-01-S1 putten – geïnterpreteerd, wat zeldzame gegevens over fractuurdichtheid, fractuuroriëntatie en de huidige spanning oriëntatie in de Nederlandse ondergrond op heeft geleverd. De gegevens benadrukken de verwachte variabiliteit in *fracture* frequentie. Het merendeel van de (open) *fractures* staat parallel aan de huidige maximale horizontale spanning oriëntatie. Uit puttestinformatie uit verschillende putten blijkt dat de variabiliteit in productiviteit van het Dinantien reservoir - indien gekoppeld aan *fractures* - aanzienlijk varieert.

De resultaten geven aan dat toekomstige activiteiten bij het schatten van de productiviteit (d.w.z. doorstroming en geothermische energie) vóór het boren een breed scala van scenario's zullen moeten gebruiken die het Dinantien *fractured* (gebroken) carbonaatreservoir kunnen beschrijven. Om zich te richten op gebieden met de grootste kans op succes moet men verschillende datasets combineren. Daarbij moeten 'sweet spots' (gebieden waar zich veel en mogelijk open *fractures*

bevinden) worden gedefinieerd door verschillende kaarten combineren die ieder een indruk geven van *fracture* kenmerken of de waarschijnlijkheid van het aantreffen hiervan. Deze kaarten kunnen o.a. aangeven waar *fractures* door verbreuking, plooiing of mechanische gesteente kenmerken meer - of minder - waarschijnlijk zijn. Statistische onderbouwing is zeer waarschijnlijk niet mogelijk daar de schattingen gebaseerd zullen zijn op zeer beperkte gegevens. Speciale aandacht moet worden besteed aan de beoordeling van de *fracture* frequentie (zie bovenstaande), de oriëntatie de huidige spanning in de ondergrond. Inzicht hierin zal de waarschijnlijk op het aantreffen van een open fracture systeem vergroten. Ontwikkelings- of exploratieconcept, putplanning en data-acquisitie moeten worden geoptimaliseerd om de kans op geothermische ontwikkeling te maximaliseren en tegelijkertijd informatie te verstrekken over de belangrijkste onzekerheden. Wellicht dat voor de *fractured* reservoirs afgeweken moet worden van een doublet, maar dat een ontwikkeling met meerdere putten een grotere technische kans van slagen heeft (niet perse een hogere kans van economisch slagen).

2 Executive summary

As the Dinantian carbonates are predominantly tight any flow from these reservoirs has to be provided by fractures and/or karst. Main questions for geothermal development are; do open fracture systems exist, how are they distributed laterally and vertically, do make up extensive network in order to produce sufficient volumes consistently and – if any – how are they oriented. Fracture characterization (e.g. orientation, size, width, frequency) is therefore an important step towards geothermal exploration and development of the Dinantian carbonates.

Fracture characteristics are influenced by various factors, like geological and hydrological history, historic and present day stress state, possibly by bed thickness, facies, lithology. Finding relationships between fracture characteristics and the factors above requires insights into the timing of each individual factor and how this influenced the fractures. This may be deduced from a combination of various data types like; high resolutions 3D seismic data, well data and production data. However, even for reservoirs with considerable amounts of high quality data the understanding of reservoir productivity and productivity forecasting can be extremely challenging. Considering this, fracture characterization of Dinantian carbonates in The Netherlands is severely hampered by the present lack of data. Therefore, any future activities on this topic will heavily rely on scenarios with wide ranges of fracture characteristics often based on limited local data and more analogue data, despite its limitations as discussed in this report. Any new well in the near future targeting the Dinantian carbonates should accommodate substantial data acquisition across the reservoir section (e.g. borehole imaging, acoustic logs, core).

This report provides a start to the characterization of Dinantian fractures. It summarizes general information on fractures, it discusses workflow activities that may be conducted in these kind of assessments, but which were not all conducted in this study, mostly due to the lack of data. References to other SCAN reports are made as well. Furthermore, the report refers to some analogue data which may be further built on in the near future. Observations that (may) indicate fracturing in Dutch wells that drilled the Dinantian are summarized from multiple sources. For this report the FMI well logs – from the LTG-01 and CAL-GT-01-S1 wells – were interpreted providing rare data on fracture density, fracture orientation and present day stress state in the Dutch subsurface. The data emphasizes the expected variability in fracture density. The majority of the (open) fractures are aligned with the present day maximum horizontal stress orientation. Well test information from various wells shows that variability in productivity of the Dinantian reservoir – if linked to fractures – varies considerably.

Results indicate that future activities in estimating pre-drill productivity (flow and geothermal power) will have to use a wide ranges of scenarios that may describe the Dinantian fractured carbonate reservoir. In order to target areas with the highest chance of success one has to combine various datasets. Thereby, ‘*sweet spots*’ have to be defined based on maps where favorable fracture characteristics are indicated to be more – or less – likely (faults, folded areas, mechanical stratigraphy, other), but without quantifying the statistics, as estimates will likely be based on very limited data. Special attention should be given to the assessment of fracture density and orientation which are likely strongly related to present day stresses. This will increase the chance of encountering open fracture systems. Development or exploration concept, well planning and data acquisition should be optimized in order to maximize the chance of geothermal development while providing information on the main uncertainties. Possibly, *fractured* reservoirs should not be developed by means of a doublet, but with multiple wells to increase the technical chance of success (not necessarily leading to an economic success).

3 Introduction

Geothermal energy systems have been considered as a potential alternative for the fossil fuel heating. Currently, there are geothermal projects already functioning in the Netherlands. However, the application of geothermal energy in existing projects is not adequate for the provision of high-temperature heat for, as an example, the process industry. It is anticipated that Ultra Deep Geothermal (UDG) energy could potentially make a substantial contribution to the transition towards a sustainable heat supply. To reach sufficiently high temperatures in the Netherlands, geothermal reservoirs at depths over 4 km are required. The Dutch subsurface at these depths has not been explored extensively until now and is therefore relatively unknown. Based on the limited amount of subsurface data, the Lower Carboniferous Dinantian Carbonates were identified by Boxem et al., 2016 as the most promising target matching the initial requirements for UDG.

The fracture characterization work reported in this document is a result of SCAN, a government funded, program to scope out the potential of geothermal energy, including from the Dinantian Carbonates. This program includes a range of subsurface studies of the Dinantian Carbonates. The results of the SCAN studies will be released and become available via www.nlog.nl/scan.

3.1 Importance of fractures for Dinantian

To exploit the geothermal potential of the Dinantian carbonates it is essential that the rock is able to flow economic volumes, consistently. Dinantian rocks are in general very tight, mostly lacking medium to high porosity matrix and having hardly any matrix permeability to allow flow through the rock (see Petrophysical evaluation (Carlson, 2019)). Therefore, it is considered that flow from the Dinantian, for most locations, has to be accommodated by (open) fractures and/or karst (if any). It is therefore vital to recognize and understand fractures zones within the Dinantian wellbores as well as being able to estimate the chance of encountering open fracture networks and their orientation for geothermal exploration and/or development wells. This is difficult for reservoirs with many wells, well logs, core and 3D seismic coverage, but is extremely challenging for the Dinantian carbonates due to the limited and scattered data. To accomplish this goal, several observations from various sources need to be integrated. These sources include:

- Seismic data (preferentially 3D seismic data to enable seismic attribute extraction);
- Well data
 - Cores;
 - Borehole images;
 - Other logs such as DSI, DT, GR, or RHOB
 - Well test data
 - Production data
- Stress maps

If these data are sparse or insufficient additional investigations may focus on:

- Outcrop analogues;
- Analogue subsurface reservoirs

3.2 This report

The aim of this report is versatile. It describes fracture basics and discusses activities that contribute to fracture characterization. Not all of the suggestions listed in this report were executed since a lot of the data mentioned above is lacking for large parts of the study area. Fracture characteristics may vary at small scale as well. As fracture density and aperture is an important input variable to estimate the flow potential estimation of Dinantian carbonates (Bruijnen, 2019), a start was made to collect this information from literature. Observations of fractures in subsurface Dinantian carbonates are mainly based on borehole image (BHI) interpretations for two wells conducted for this study. The BHI interpretations provide rare data points on present day stress orientation data and have also been used in the stress mapping study which is published in a separate document (Osinga & Buik, 2019).

The geology of the Dinantian carbonates and of the overburden are described in detail in the SCAN report on Facies analysis and diagenetic evolution of the Dinantian carbonates in the Dutch subsurface (Mozafari et al, 2019).

4 Fractures

Fractures are separations within a hard rock dividing the rock and are commonly caused by stresses that exceed the rock strength. Fractures exist everywhere in the subsurface (Nelson, 2001). The stresses are exercised during burial and tectonic events like crustal extension and compression. When no displacement can be observed between the two fracture walls the fractures are referred to as tensile fractures, joints or fissures. Filled joints and fissures are referred to as veins. Whenever slip or shear along the fracture plain is observed one speaks about shear fractures. Shear fractures have generally lower angles than the tensile fractures.

Fractures that cross each other, typically not perpendicular, are referred to as conjugate fracture sets (Figure 1). Fractures or joints can be open or closed which is often related to the present day stresses, pressures and/or precipitation of minerals or sediments within the fracture aperture. In general, fractures are believed to close as the stresses on the fracture increase with increasing burial depth. However, fractures can remain open due to various conditions; 1) As the fracture plane is seldomly smooth (see Figure 2), minimal amounts of shear could actually prevent the fracture from closing when stress is increased (Bisdorf et al, 2016) as the planes do not fit perfectly together (see also section 4.2.1). 2) Whenever fluids in the fractures cannot escape when stress on the fracture is increased the fluids can prevent the fractures to close. As a result the fluid pressure increases above the previously hydrostatic state and the reservoir is referred to as being over-pressured. This overpressure can be released during fluid escape events which can in itself create new fractures which could be filled again with clasts from the host rock (see Figure 23). 3) Hydrothermal diagenesis can result in widening of existing fractures.

In general fracture presence and characteristics are heavily controlled by the (hydro-) geological history of the host rock and the composition of the host rock itself. This results in a very heterogeneous systems which is difficult to describe with subsurface data alone. Often field studies of outcrop and various analogues with similar kinds of lithology, structural styles or basins are used to complement the

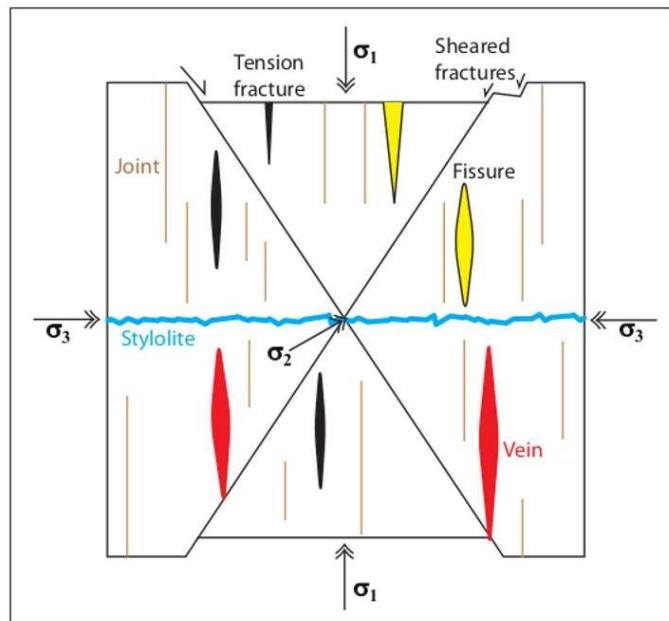


Figure 1: Schematic overview of fracture nomenclature. The crossing fractures are called conjugate fractures. (from GEO Education)

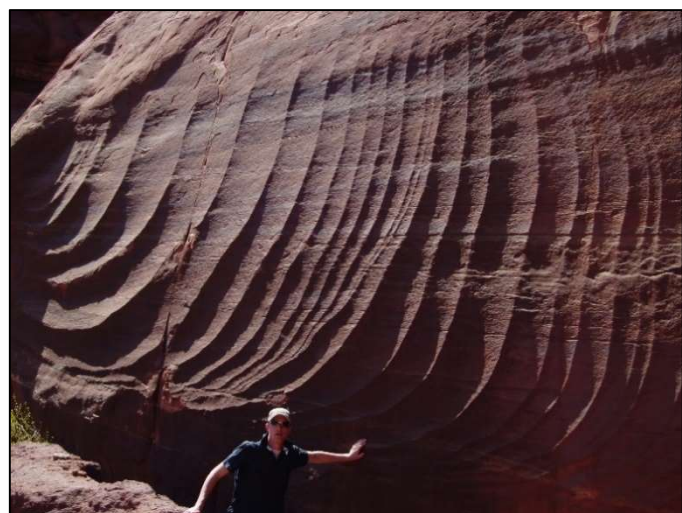


Figure 2: Picture of a fracture plane of a 'plumose' fracture that originate from a single point. Example is from a sandstone formation, Utah.

subsurface data although this approach brings its own biases and uncertainties as well (described in Chapters 5 and 6).

Stylolites in carbonates are often referred in literature to as a type of compressional fracture. They exist as irregular surfaces perpendicular to the maximum stress orientation and are a result of compaction and dissolution. If the host rock in which stylolites have formed contained clastic material this can have accumulated in the stylolite resulting in either baffle to or conduits for fluid flow. Stylolites have not received detailed attention in this report, but may be considered when connectivity is discussed.

4.1 Fractured carbonate reservoirs

Within a rock the matrix porosity and the associated permeability (the ability of fluids in the rock to flow) determine whether fluids may easily flow through the rock or not. Open fractures may provide (better) flow conduits through the rock for fluids as they connect to matrix porosity and/or by linkage of multiple fractures and joints which create fracture networks (see Figure 3). Closed/cemented fractures may, however, act as effective flow baffles (Laubach (2003), Laubach et al. (2019)). Secondary dissolution of cemented fractures and veins may result in vuggy fracture porosity that can potentially contribute to flow again as well. A nice core example is published in Van der Voet et al (*in press*) (see Figure 4 and Figure 23).

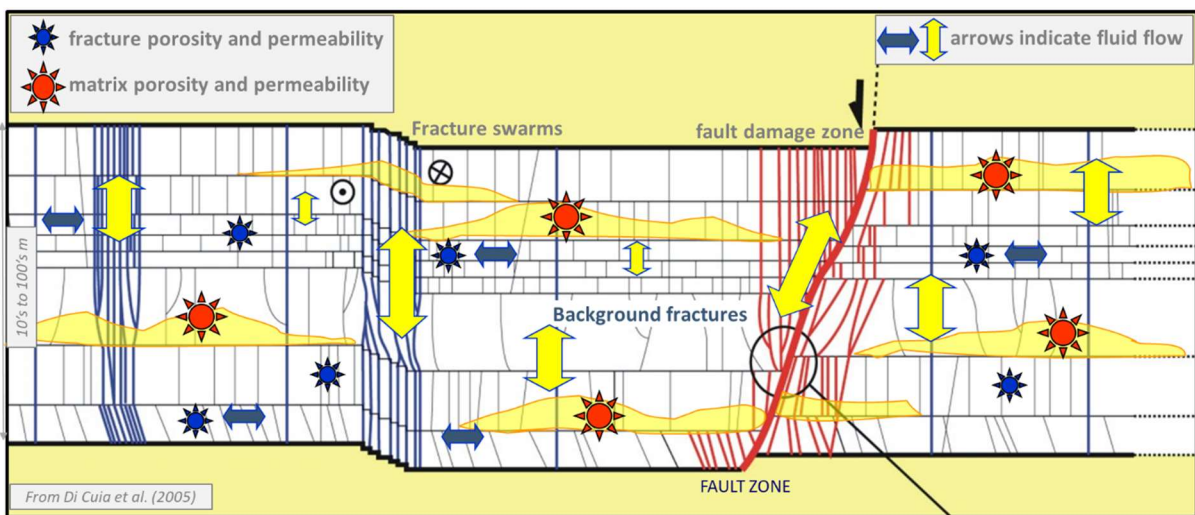


Figure 3: Schematic representation of different flow elements (matrix, elements, faults) and their potential interaction (modified from Di Cuia, 2005).

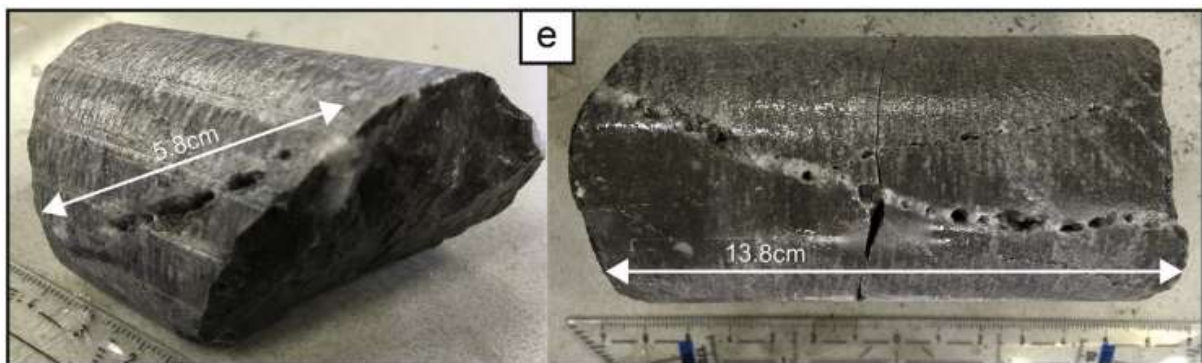


Figure 4: Vuggy fractures in Dinantian carbonates from Heibaart DZH1 borehole (Van der Voet et al, *in press*)

Quantitative elements for flow estimation are – among others – the fracture spacing and fracture aperture. Fracture spacing is the distance between individual fractures. Its inverse – and more often used term – is the fracture density/frequency which is expressed as the number of fractures per – typically – foot or meter. The fracture aperture describes the distance between the two wall surfaces on either side of the fracture. These two variables contribute to a large extent to an estimate for the fracture permeability (or fracture porosity) across the entire reservoir (see also Bruijnen, 2019).

The relationship of how much flow from a reservoir originates from matrix versus fractures results in roughly four classes (Figure 5, Nelson (2001)). Dinantian carbonates are generally very tight (low permeability) and have low porosity and would therefore likely classify as a type I or II reservoir. Although presented in a simple diagram the rock matrix and fracture interaction and associated fluid flow is complex and often difficult to predict.

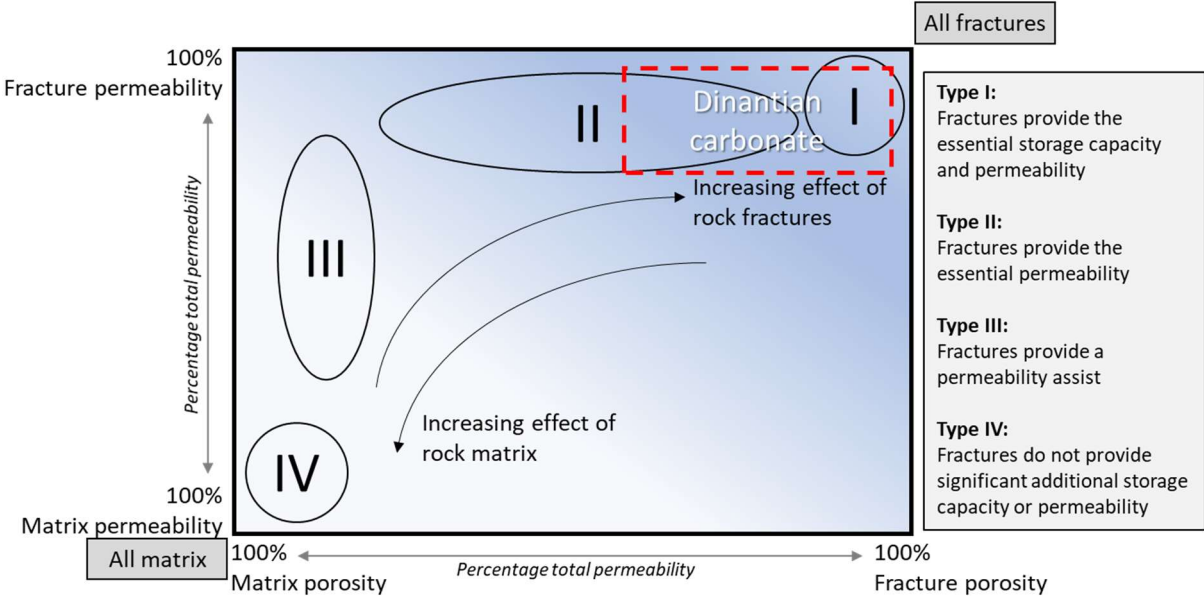


Figure 5: Fracture classification modified from Nelson (2001). According to the figure reservoirs can be roughly classified into four classes based on the contribution of matrix versus fractures to the reservoir storage and permeability. Dinantian carbonates are typically tight (low permeability) without a lot of porosity and that would result in a type I – II classification.

As fractures and fracture networks may allow fluid flow these features can also eventually contribute to (sub-) surface erosion and leaching (dissolution) of the rocks. This may eventually result in the formation of caves or so-called karst (Klimchouck et al., 2016). Karstification that is not related to near surface hydrological processes is more often referred to as hydrothermal karstification. Karst features both near surface and at greater depth may collapse. Often the karst is being filled with debris from the host rock in which the karst formed and sediments that are deposited at the time of collapse or were already deposited above. The chance of open karst systems being preserved in the subsurface is decreasing with depth.

For drilling operations (open) fracture systems may cause serious issues with either losses, gains (in over-pressured systems) or well bore stability.

4.1.1 Flow enhancement of carbonate reservoir

Besides the naturally occurrence of open fractures these can be created by actively stimulating the rock, which is better known as ‘fracking’. Mixtures of water, gels and particles (proppant) are pumped through a wellbore until the host rock breaks and a fracture will be created. The fracture will be filled by the mixture is propagated when pressure is being maintained. The proppant is used to

maintain an open fracture after the pumping is stopped. While the proppant remains in the reservoir the fracking fluids will deteriorate and produced back to surface via the wellbore.

Fracking of a carbonate host rock can be combined with pumping acids into the newly created fractures. The acids will dissolve the carbonate rock thereby enlarging any fracture or matrix porosity. It will also increase the roughness of the fracture walls (make it more irregular and less smooth). This roughness may ensure that even when the fracture closes over production lifetime the fracture will remain a degree of permeability as the fracture walls do not perfectly fit together any longer. Acid treatments can also be performed as a standalone operation - without the fracking. In this case the acid will only affect the rock nearest to the well bore and may only enter pre-existing fractures.

4.2 Fracture aperture

As previously mentioned, both fracture aperture and density are considered important fracture characteristics which affect the productivity of the reservoir. It is also an important input parameter in the numerical and analytical models used to estimate potential Dinantian productivity (Bruinen, 2019). Because fracture apertures were not measured on core nor from FMI in this study a start was made to collect data on fracture apertures from available literature. In the last few decades a considerable amount of effort has been put into the in-situ measurement of apertures of fractures. Permeability in a fractured system is heavily dependent on the hydraulic aperture of fractures, since it is proportional to the third power of the aperture (Van Golf-Racht, 1982). This can be demonstrated when a fracture is considered as two smooth parallel plates in which laminar viscous flow occurs (Figure 6).

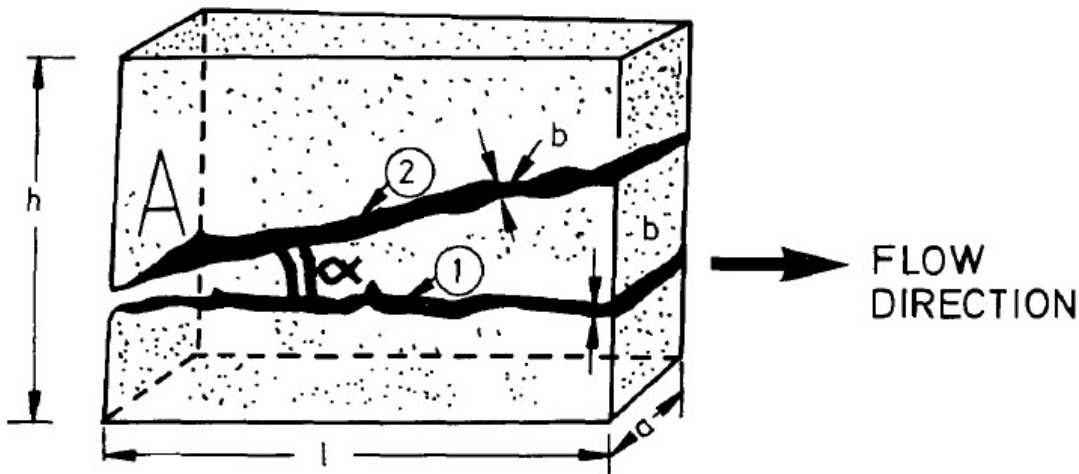


Figure 6: Matrix block containing a single fracture, parallel to flow (Fracture 1) or at an angle α (fracture 2) (Van Golf-Racht, 1982).

For an angle $\alpha=0$, the intrinsic fracture permeability, K_{ff} , is proportional to the square of the aperture b :

$$K_{ff} = \frac{b^2}{12}$$

If the angle α is not zero, a correction factor of $\cos^2\alpha$ must be applied.

The more conventional *effective fracture permeability* K_f , based on the classic Darcy definition, considers the fracture and the associated rock bulk as one hydrodynamic unit. This is expressed as:

$$K_f = \frac{b^3}{12h}$$

It is clear that the effective fracture permeability K_f scales linearly with fracture intensity (number of fractures per meter, the inverse of the fracture spacing h), but more importantly, that it is proportional to the third power of the aperture. Table 1 shows a calculation of fracture permeabilities, both intrinsic and effective, for apertures ranging from 1 to 1000 micrometer. Fracture spacing in this example is 1 fracture per meter. An average fracture aperture of 50 μm results in an effective permeability of 10 mD, whereas an average fracture aperture of 500 μm would result in an effective permeability of 10 Darcy!

It is therefore of utmost importance to have good measurements of the fracture apertures in the reservoir.

Table 1: Calculated fracture porosities (ϕ_f), intrinsic (K_{ff}) and effective (K_f) fracture permeabilities for various fracture apertures b , using parallel fractures with a spacing of 1 fracture per meter.

b (μm)	K_{ff} (μm^2)	K_{ff} (mD)	ϕ_f	K_f (mD)
1	0.08	82	1.00E-06	0.00008
10	8.3	8,167	1.00E-05	0.08
20	33	32,667	2.00E-05	0.65
50	208	204,167	5.00E-05	10
100	833	816,667	1.00E-04	82
200	3,333	3,266,667	2.00E-04	653
500	20,833	20,416,667	5.00E-04	10,208
1,000	83,333	81,666,667	1.00E-03	81,667

Unfortunately, direct, in situ measurements of fracture apertures in the borehole is very difficult, if not impossible. One has to resort to indirect methods (wireline logs or other geophysical methods) to assess the apertures. Further complications arise from the fact that many natural fractures can be assumed to have been enlarged in the vicinity of the borehole because the mudweight normally exceeds the pore fluid pressure. So regardless of the accuracy of the method employed, hydraulic apertures obtained from measurements in the wellbore are only first-order approximations (Luthi & Souhaité, 1990).

Several methods have been proposed to estimate fracture apertures:

- Direct measurement on cores (e.g. from whole core photographs);
- Difference between LLD/LLS and RXO (Sibbit & Faivre, 1985);
- Reflected Stoneley wave arrivals (Hornby et al, 1989);
- Electrical currents, generated by borehole image pads (Luthi & Souhaité, 1990);
- Mud losses (Lietard et al, 1999, 2002; Huang et al, 2011)
- Reverse engineering from well productivity (Freites et al, 2019)

For fractures in outcrops, some additional methods have been employed:

- Direct measurement on outcrops;
- Magnetic resonance imaging (MRI) on epoxy replicas of outcrop fractures (Renshaw et al, 2000);

- Spectrophotometric analysis (SA) of epoxy replicas of outcrop fractures (Renshaw et al, 2000);

Every method has its advantages and disadvantages. We will not discuss apertures of fractures in outcrops here, as they are not considered representative of those in the Ultra Deep Geothermal realm, the subject of the current study.

Direct measurement on core suffer partly from the same problem as outcrops. The moment a core is brought to the surface, it will decompact due to the release of confining and pore pressure on the sample. In addition, decompaction will likely start at the open fractures, because they are easiest to expand.

4.2.1 Factors that influence fracture apertures

4.2.1.1 Effective stress

Fracture apertures are a result of the effective stress exceeded on the fracture. Fracture aperture decreases under increasing compression, and the permeability decreases because of the smaller cross-sectional flow (Walsh, 1981). With increasing compression the number of points of contact between the fracture surfaces also increases, which causes the flow path to be more tortuous. This effectively reduces the fracture permeability further.

On the other hand, an increase in fluid pressure causes the fracture to open, thereby increasing the permeability. It also causes a decrease in the number of contact points between the fracture surfaces, which increases the permeability further due to a lower tortuosity.

Walsh (1981) derived an analytical relationship between effective stress and fracture permeability, and found that the cubic root of the fracture permeability was linearly related to the natural logarithm of the effective stress. The effective stress (or pressure) is defined as

$$p_e = p_c - sp_p$$

where p_c is confining pressure, p_p is pore pressure, and s depends on the topography of the fracture surfaces and rock type. This theoretical relationship coincided very well with experimental results obtained by e.g. Brar & Stesky (1980), see Figure 7.

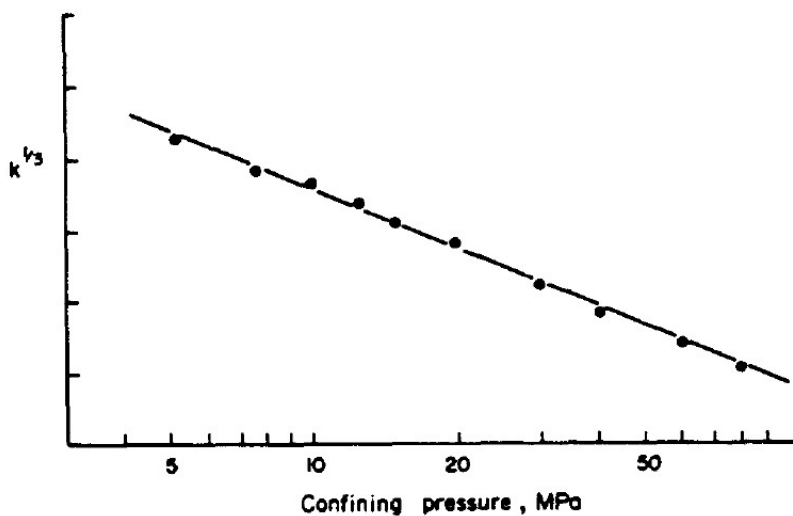


Figure 7: Hydraulic aperture decrease with increasing effective pressure. Flow data from experiments by Brat & Stesky (1980).

Other experimental data were obtained by Hakami (1989), who used epoxy casts of fracture surfaces to determine detailed fracture surface topography and hydraulic aperture distributions. Although the setup of the experiments did not allow for a quantitative relationship of fracture aperture and effective pressure, a qualitative analysis of a single fracture showed a conspicuous decrease in aperture distribution (Figure 8).

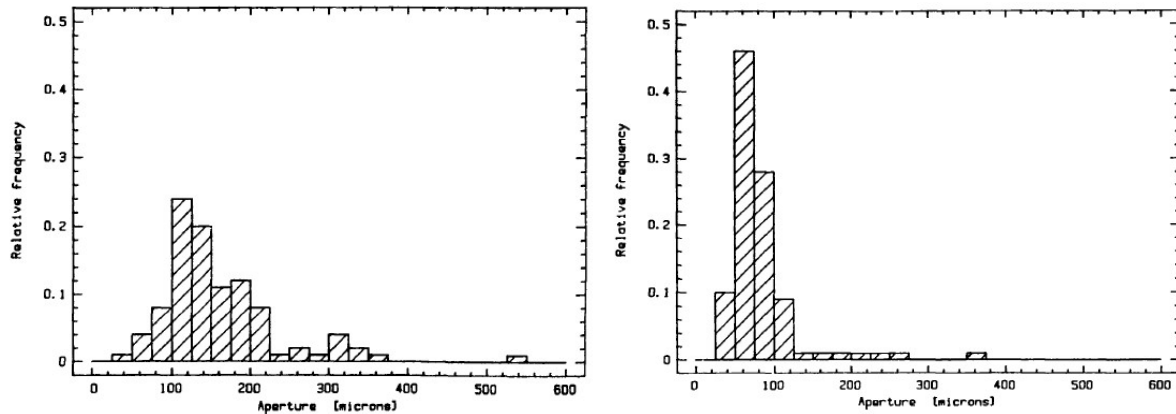


Figure 8: Aperture distribution of a single fracture measured at zero normal stress (left) and at several MPa (right). From Hakami (1989).

Bandis et al (1983) did extensive laboratory experiments of the deformation characteristics of rock joints under normal and shear loading. They developed quantitative relations between normal deformability and relevant joint parameters (aperture, wall strength and roughness). For natural interlocked (mated) joints – joints will perfectly fit together when compressed – they suggested a hyperbolic function to describe the stress-closure opening curves, whereas dislocated (unmated) joints were best described by a semilogarithmic function.

In rare cases a decrease in effective stress can actually increase fracture permeability in due time. A prime example is the fractured carbonate field Le Lac in the Aquitaine Basin, France. Production data from Le Lac showed that the field’s permeability had increased during its productive life while depleting (Rolando et al, 1997). The explanation is that during production of the gas the pore pressure decreased to such an extent that small rock movements occurred along the fractures, causing the two surfaces of a fracture not to fit together completely anymore (they effectively become unmated), thereby increasing the aperture and thus the permeability.

Present day stress is believed to be an important factor on the variation in fracture aperture. There are however multiple examples where the orientation and location of open fractures is different from the present-day effective stress regime (Laubach, 2003).

4.2.1.2 Diagenesis

Fracture aperture can be significantly enhanced or reduced by diagenesis. Fractures that were originally open may get partially closed as a result of cementation and act as flow baffles (Laubach, 2003). On the other hand, secondary dissolution of cemented fractures and veins may result in vuggy fracture porosity, thereby greatly enhancing the permeability (Figure 4; Van der Voet et al., 2020). This is also observed in Dutch Dinantian cores (Mozafari et al., 2019).

4.2.2 Data on fracture apertures

Data from several sources have been compiled to arrive at an estimate of the likely extreme values for fracture apertures in the Zeeland Formation. Most data sets have been compiled from literature on existing fields. The methods that were employed to estimate the fracture apertures have been noted where possible. One dataset was compiled by the authors (Table 3), but for further studies it is recommended to enlarge this dataset with other available data. It must however be stressed that specific data on sizes is sometimes hard to come by and also the fact that apertures are measured on different datasets (e.g. outcrop or BHI logs) will possibly not reduce the range of uncertainty. Furthermore, as also discussed in this report fracture characteristics are very site specific mainly due to its relation to the hydro-geological processes through time. This makes extrapolation or selecting the 'right' analogue nearly impossible. As a result large ranges will remain and scenarios will need to be used covering this range.

Van Golf-Racht (1982) presents a dataset that ranges from 0 to 150 microns (Figure 9), but the exact origin of the data is not clear. In the description he states *"The fracture width varies between 10-200 microns, but statistics have shown that the most frequent range is between 10-40 microns"*. (Table 3)

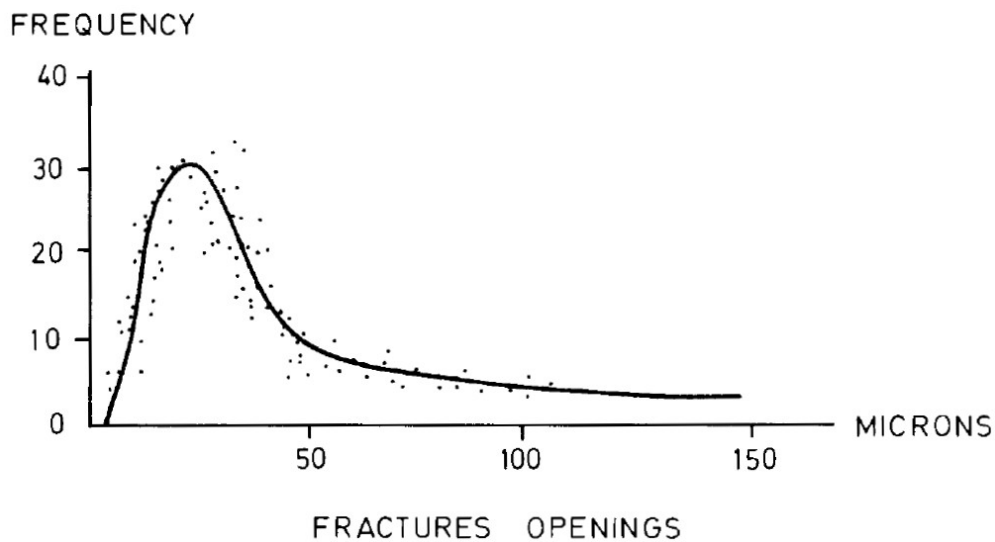


Figure 9: Statistical frequency of opening width of fractures (Van Golf-Racht, 1982).

Data from a fractured carbonate oil field situated in Central Asia . The reservoir is a bioclastic limestone of Lower Carboniferous age. It lies at a depth of approximately 3000 m. Production is from fractures and matrix. On a total of more than 100 wells drilled in the field, 37 had borehole images. 13 of these had a fracture aperture analysis done, and were included in the following discussion. A total of 5572 conductive fractures had been picked (Figure 10) and their hydraulic apertures calculated according to the method of Luthi & Souhaité (1990). Figure 10 shows the results: apertures range from 0.5 to 400 microns, and the median value is 5 micron.

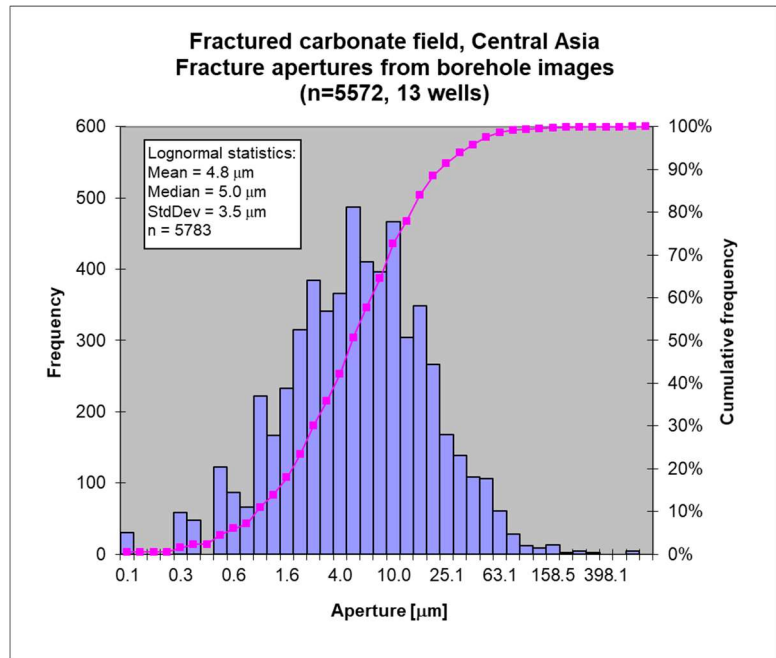


Figure 10: Fracture apertures derived from FMI from a Lower Carboniferous fractured carbonate field, Central Asia.

In 1987 a research well in Moodus, Connecticut, was drilled into metamorphic and igneous basement rocks to study the state of stress in an area known for shallow earthquakes. The fractures in this well have been extensively investigated and described (Luthi & Souhaité, 1990; Plumb & Hornby, 1988). Figure 11 shows the fracture intensity and the fracture apertures in this well as measured by Zoback & Moos (1988). Average fracture aperture is about 2 microns, and the largest ones have an aperture slightly over 20 microns.

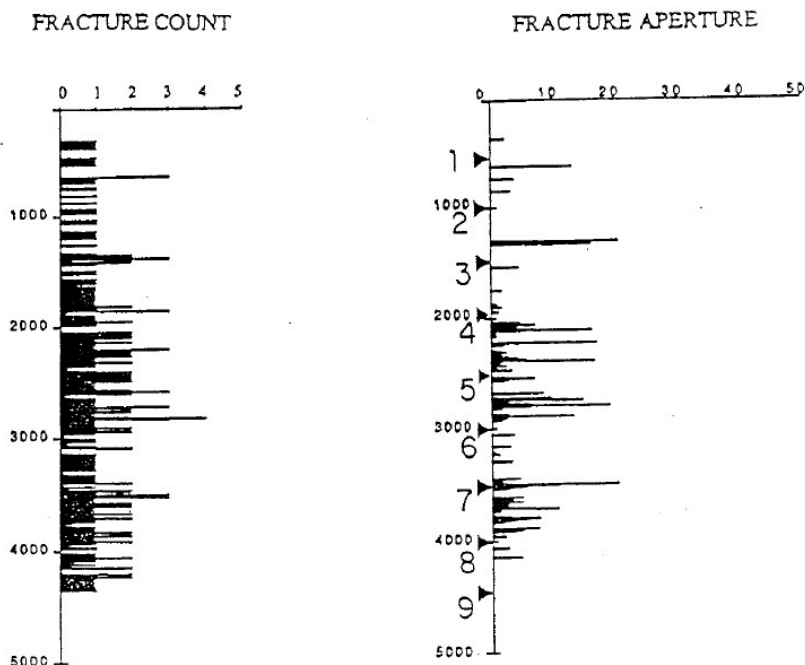


Figure 11: In Situ Fracture Count and Aperture in a research well in Moodus, CT (Plumb & Hornby, 1988). Depths are in feet size in microns.

A specific example of fracture apertures of the Middle Cretaceous Basquiria Limestone is given by van Golf-Racht (1982). Table 2 lists the distribution of the hydraulic apertures. The average aperture is 79 microns.

Table 2: Opening widths from Basquiria Limestone, Middle Cretaceous (modified from: Van Golf-Racht, 1982).

Class of width (mm)	Average width (mm)	Number	Frequency (%)
<.01	.01	430	39%
.01 – .03	.02	80	7%
.03 – .07	.05	180	16%
.07 – .13	.10	270	24%
.13 – .17	.15	10	1%
.17 – .23	.20	20	2%
.23 – .27	.25	30	3%
.27 – .33	.30	60	5%
.33 – .67	.50	30	3%

Although no tabulated values for fracture apertures are given Luthi & Souhaité (1990), a rough idea of the distribution of apertures can be obtained if the illustrations of the interpreted borehole images are studied. More than half of the fractures have apertures of less than 40 microns, and none of the fractures has apertures wider than 600 microns.

4.2.3 Summary

The overview of the different datasets described above is presented in one table and a table from Nelson (2001) is added to it (Table 3). A large variation in fracture aperture exists, but the majority of these datasets indicates that fracture apertures are more likely tens of microns than hundreds. Of course can chemical alteration (diagenesis) and over-pressured systems enlarge or maintain fracture widths. However, the same factors may also cause the fractures to close, along with increased stress with burial. However, a lot of the data is gathered from outcrops which are difficult to translate to subsurface conditions (rationale discussed in Chapter 6.1). FMI data of the Mol geothermal wells may indicate an average fracture width of 170 microns (3000 – 3600m TVD) (see Chapter 6.3.2.3).

Table 3: Summary of data sets with reported fracture apertures

Data set	Reference	Depth [m]	Age & lithology	Method	Nr of fractures	Avg. aperture [μm]	Max. aperture [μm]
Various	Van Golf-Racht (1982)	“Reservoir depth”	Unknown	Unknown	1000’s	20	120
Central Asia	Proprietary TNO report	3000	Lower Carboniferous carbonates	Borehole images – Luthi-Souhaité method	5583	5	500
Basquiria Limestone	Van Golf-Racht (1982)	unknown	Middle Cretaceous Limestone	Unknown	100’s	79	670
Moodus well, Connecticut	Zoback & Moos (1988)	0-1500	Paleozoic metamorphic & ignous		10’s	3	25
Moodus well, Connecticut	Luthi Souhaité (1990)	0-1500	Paleozoic metamorphic & ignous	Borehole images – Luthi-Souhaité method	10’s	~50	>100
Noorishad and others (1971)	Nelson (2001)	-	-	-	-	3000	-
Ohnishi and Goodman (1971)	Nelson (2001)	-	-	-	-	1300 – 2500	-
Sharp and others (1972)	Nelson (2001)	-	-	-	-	100 – 500	-
Snow (1968a)	Nelson (2001)	-	-	-	-	5000	-
Snow (1968b)	Nelson (2001)	-	-	-	-	50 - 150	-
Van Gold-Racht (1982)	Nelson (2001)	-	-	-	-	10 – 40	-
Wilson and Witherspoon (1970)	Nelson (2001)	-	-	-	-	2500	-

4.3 Fracture density

Fracture density is a very important parameter to estimate potential flow from the reservoir. Not only is the chance of encountering open fractures larger it also increases the chance that fractures link up to create a fracture network (Figure 13). It is one of the key reservoir variables in flow estimation for the Dinantian (Bruijnen, 2019). Fracture density is dependent on many aspects like proximity to faults and other structural styles, lithology, mechanical behavior of the bedrock including bed thickness. The number of relationships makes it also very complex to derive unique correlations.

Fractures and joints can exist anywhere in the host rock, but often rocks are more heavily fractured in the vicinity of faults and are part of the so called damage zone (Figure 14). Fault damage zones exist in extensional, compressional and strike-slip settings. Compressional and strike-slip settings can create both extensional and compressional fractures (open-closed). Choi et al. (2016) provide a comprehensive overview the fault related damage zone architecture. Damage zones width shows – in general – a positive correlation with fault displacement, but the bandwidth of this correlation is wide. As damage zone in the subsurface are difficult to nearly impossible to define based on seismic data, scaling laws are generally applied (TerHeege et al., 2018). Based on Choi et al. (2016) one has to conclude that fault damage zone are most likely limited to below 100m width and more often even below 30m, moreover, this width is not constant along the length of the fault plane.

Folds and curvature of the reservoir can also lead to increased fracturing. Within the same structure contain both extensional and compressional fractures may exist (Figure 12; Cosgrove, 2015).

Mechanical rock characteristics or mechanical stratigraphy are most likely important in relation to fracture density and fracture size. Variations in clay content, texture, porosity, lithology, bed thickness etc. can play a role in how far the fractures extend or how frequent they occur (De Keijzer et al.

2007). In general, harder rocks, and therefore any component that hardens rocks, tend to be more susceptible to fracturing (Nelson, 2001). Although also thinner beds tend to fracture more often (Bai

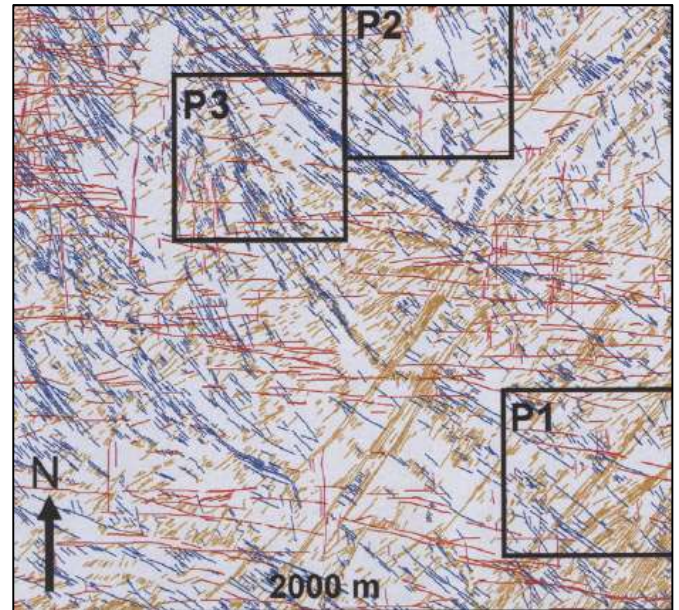


Figure 13: Example of variation lineaments and therefore fracture networks in Cretaceous carbonates from a field study in Oman (De Keijzer et al. (2007)

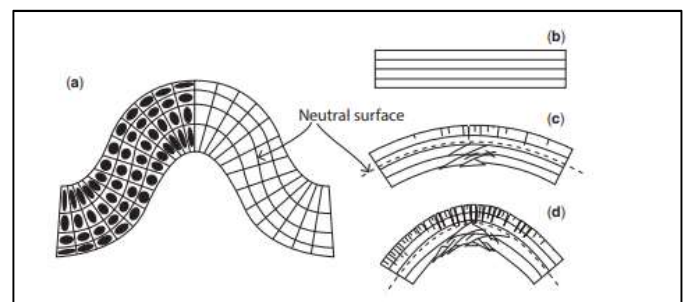


Figure 12: Schematic display of folded structure indicating compressional and extensional regimes throughout the structure leading fracturing. (Cosgrove, 2015 who used it from Ramsey, 1987)

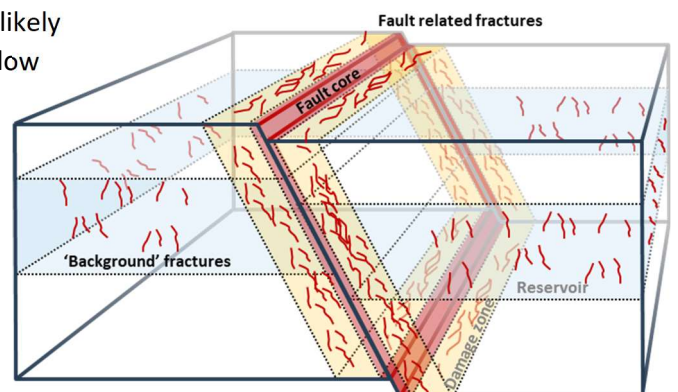


Figure 14: Schematic impression of 'background fractures' and fault related fractures.

& Pollard (2000)). This seems to depend on the lithology as well (see Figure 15). Outcrop images in Poty (2006) (see Figure 17) seem to be in line with the thinner beds, more fracture statement while in the Heibaart DZH1 well in Belgium (subsurface!) fractures are found to be more frequent in the massive reefal buildups (Van der Voet et al., 2020). Moreover, even more important are the fractures that cross bed boundaries thereby increasing the chance of connectivity between various layers. Nelson (2001) summarizes various components that influence the fracture density (see Figure 15, Figure 18, Figure 16). Dolomite content is an interesting factor because strong variations in dolomite content within the Dinantian in The Netherlands can be deduced from the well logs that have been interpreted by Carlson (2019). However, timing is of the utmost importance as diagenetic processes, like dolomitization, can be pre- or post-dating fracturing events and vice versa. Present-day relationships may therefore give false correlation or the correlation that was in fact present is no longer clear.

The dependency of fractures on rock properties does result in vertical variation. This partly explains the variation seen in the LTG-01, CAL-GT-01 and Heibaart DZH1 wells. Even when mechanical rock properties would not vary laterally, still lateral variation in fracturing has to be expected. As mentioned fracture corridors or swarms form, but not exclusively, near faults as part of damage zones.

Implications for the chance of encountering fractures in the Dinantian are that one has to target faulted or folded areas within layers that have preferentially been fractured.

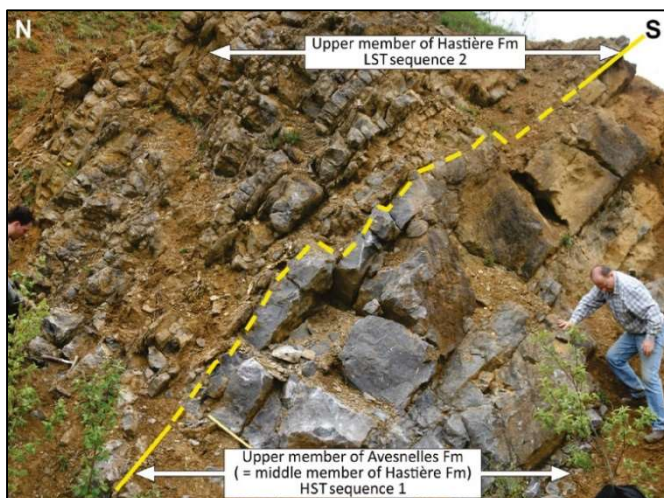


Figure 17: Picture from Poty (2016). Although not the purpose of this picture it nicely shows that fracturing in thinner beds (left/above of yellow line) is more dense than fractures in the thicker beds.

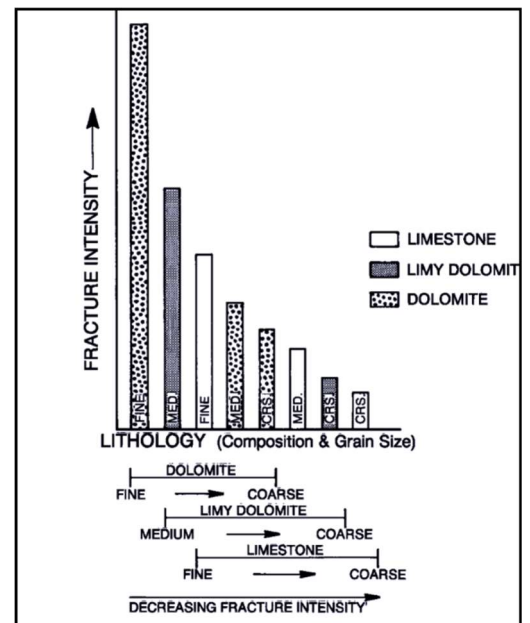


Figure 15: Relationship between fracture density (intensity) and lithology (Nelson, 2001).

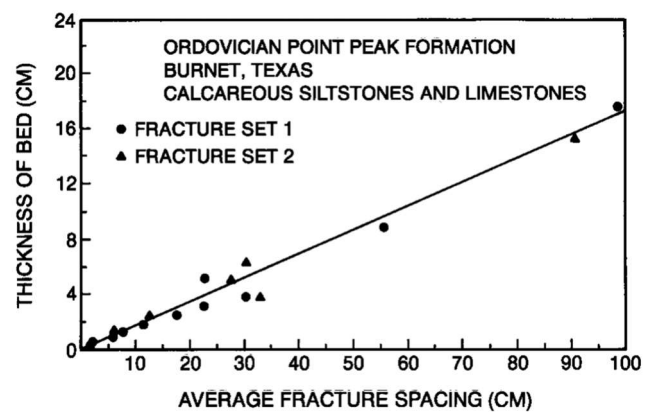


Figure 16: Relationship between fracture density and bed thickness (Nelson, 2001).

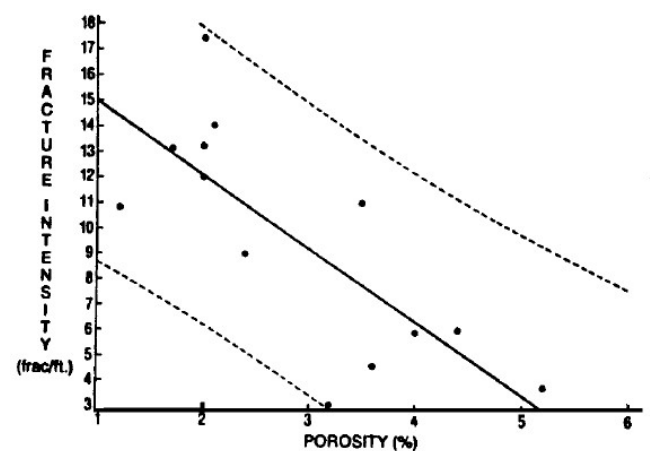


Figure 18: Relation between porosity and fracture density for a Lower Paleozoic dolomite (from Nelson, 2001).

5 Fracture characterization components and implications

To exploit the geothermal potential of the Dinantian carbonates it is essential that the rock is able to flow economic volumes, consistently. Fractures will play an important if not the most important role in order to extract geothermal energy from Dinantian carbonates. Fractures are however also related to safety aspects like drilling hazards and induced seismicity.

The presence of fractures is certain. However, the fracture density and whether these fractures are open and connected to form fracture networks is and will remain a large uncertainty. One has to combine a variety of (analogue) data in order to develop conceptual reservoir models or scenarios. These conceptual models have to be location specific as variations in subsurface conditions across The Netherlands exist due to differences in geological history. However, the lack of data will imply one has to build for a large part upon regional studies and various analogues. A series of activities is described below which helps to build the picture of the fracture specifics, especially when they are combined. If data is sufficient, probability maps may be created to indicate areas that are more or less favorable for finding permeable reservoir. This was not done for this report for several reasons, but mainly because fracture characteristics show a large variation between different locations. Therefore, the maps require a lot of local detailed data or interpretations for which no sufficient datasets are available (e.g. large areas in The Netherlands lack high quality 3D seismic data for the Dinantian interval). However, these maps could – for example – indicate:

1. Probability of the presence of fracture corridors;
2. Probability of the presence of open fractures (e.g. due to recent tectonic activity);
3. Probability of the presence of open fractures due to their orientation parallel to the maximum horizontal stress direction;
4. Probability of the presence of a geomechanical facies favorable for the formation of fractures

These maps could then be combined with maps from other datatypes and disciplines:

1. Curvature maps, indicating different degrees of folding of the strata
2. Probability of the presence of karst
3. Probability of matrix porosity & permeability
4. ...

5.1 Seismic interpretation

Seismic data may help to understand the structural setting. Detailed seismic interpretation of faults is essential to highlight areas of increased fracturing as part damage zones, but will not reveal the fractures itself nor its conductivity to fluids (see Table 4). High resolution mapping of the top structure – in case of 3D seismic data availability – will highlight areas with more curvature and increased curvature may have a positive effect on fracture density and aperture. Examples of fault interpretation, using a variety of attribute toolboxes, are given in the SCAN seismic interpretation report (Ten Veen et al., 2019). Similar exercises need to be conducted for other areas of interest, but requires good quality 3D seismic data which is currently lacking for most of the Dinantian carbonates in the Netherlands. If such data would be available, seismic inversion studies may provide information on rock mechanical behavior which may directly affect fracturing (see also below). Proper calibration well data (including Vp/Vs data) is currently extremely sparse leaving – again – lots of uncertainties.

Wells penetrating the Dinantian carbonates in the Netherlands were mostly drilled on or close to 2D seismic data. However, the absence of good quality 3D data may also result in difficulties explaining

production behavior of wells and to assess possible negative effects of geothermal operations like induced seismicity (see also Buijze et al, 2019).

Table 4: Comparison of different scales between fractures and faults. (figures are indicative)

Feature	Horizontal	Vertical	Throw
Seismic faults	500 m – 10 km	100 m – 1 km	10 m – >1 km
Sub-seismic faults	100 m – 1 km	50 m – 500 m	0 – 20 m
Fracture corridors	10 m – 1 km	10 m – 100 m	0 – 1 m
Fractures or fissures	1 cm – 10 m	1 cm – 10 m	0 – 1 m
Micro-fractures	1 mm – 1 cm	1mm – 1 cm	0

5.2 Tectonic evolution

Timing of past tectonic movements in combination with past and present day stress magnitude and orientation in combination with timing of diagenesis may point to preferred fracture orientation and the likelihood of fractures being open. This will at best result in *more likely* or *less likely* statements. As part of the SCAN studies, a reconstruction project was conducted along 2 transects across The Netherlands, indicating where, when and how areas have been tectonically active. This work is reported in Bouroullec et al, 2019. In general, fractures that have been opened due to tectonic events may close when stresses change (e.g. during burial) or may be filled by cements through diagenetic processes over time. Therefore, areas with relatively recent tectonic movement are more likely to contain open fractures. In addition, analyses such as clumped isotopes (e.g. Dennis et al., 2019) of fracture cements may help to constrain at what temperature and depth the cements were formed. This may help to identify the window in which the fractures may have been open. These analyses have not been conducted in this study.

5.3 Present day stress field

Present day stresses are important as they may determine which fracture orientations may still be open to flow. This will directly influence the development concepts. Stresses are mapped by the SCAN stress field characterization report (Osinga & Buik, 2019). Drilling-induced fracture orientations that have been identified from borehole image logs (this report) helped to constrain present day stress orientation.

5.4 Rock mechanical properties

Rock (mechanical) properties of the aquifer are important as they may – among others – control fracturing. The Dinantian carbonates lithology and petrophysical properties have been summarized, evaluated and reported in studies by Reijmer et al (2017), Mozafari et al (2019), and Carlson (2019). Naturally, well data is essential, but limited. Borehole image interpretation in the current report completes the analyses of Mozafari et al (2019) and Carlson (2019) by highlighting bedding, textural observations and fracture mapping providing insights into vertical variation in fracture density and its nature (open, closed, orientation, dip). Vertical variation of the rock properties and – consequent – variation in fracturing impacts also well positioning considerations. It should be considered that lithology variation is sometimes caused by diagenetic processes. Therefore, the timing relation of fractures with diagenesis is very important. This also counts for using field measurements of fractures.

5.5 Flow estimation

Flow estimates for fractured reservoir are based on a variety of fracture (-network) characteristics. Flow potential for the Dinantian carbonates has been estimated in Bruijnen (2019). Fracture variables that were used in the workflow are fracture density and fracture aperture. Although the FMI interpretation gives an idea of possible fracture densities for two locations it is just a sample from a variety of possible results. Fracture apertures have not been evaluated from the FMI as the method can result in overestimation (Davatzes & Hickman, 2010). Both fracture density and fracture aperture data can be complemented by literature and analogue studies and a first pass has been conducted and listed in this report.

Production from fractured reservoir changes the behavior of the fractures e.g. fractures may close when pressure is decreased and thereby decrease in permeability (Ter Heege et al, 2018). This effect may have been observed by the CAL-GT-01 and CAL-GT-02 wells where well test productivity indices decline over time (Carlson, 2019 (evaluation CAL-GT-01 and CAL-GT-02)). This effect should be considered as well, but has not been the scope of the current SCAN reports.

Injection into a reservoir can also change the flow behavior of the rock due to the thermal effect on stress. Fractures may be created which thereby would enhance the injectivity. Literature describing this phenomenon for various types of reservoirs have been listed in a TNO report on this topic (Veldkamp et al., 2016). This effect may depend on well orientation as well in the case of horizontal wells (Hals & Berre, 2018).

5.6 Development considerations

Various considerations have to be made to develop fractured reservoirs. For a geothermal development pressure communication between wells is of key importance. Pressure communication between wells ensures that water cannot only be produced, but also injected within given (legislative) constraints (e.g. maximum allowable injection pressure). Wells need to be designed to maximise the chance of encountering fracture networks. However, geothermal developments require – at least – two wells. This means that not only the chance of drilling through open fracture systems is important, but also the chance that the drilled fracture systems in both wells are connected to each other in order to allow pressure communication.

This is visualized in Figure 19 where two situations for a doublet with two horizontal wells is visualized. At the left the wells are assumed to have drilled perpendicular through various fracture systems. While the producer well (red) penetrated fracture system [A] and [B] the injector well (blue) penetrated fracture systems [C], [D] and [E]. In this hypothetical setting only [A] and [C] would be connected which would therefore would have to accommodate all the flow required for production. There is an increased chance that, for this specific scenario, the flow rates may not be sufficient for an economic project compared to a scenarios where all encountered fracture networks would be connected. To maximize the chance of encountering several connected fracture networks the length of the horizontal well has to be balanced versus cost, risk, reward.

In the right scenario the geothermal doublet is drilled through a fault and associated damage zone, hoping to have a higher chance of encountering open fractures (and possibly associated karst). Even though the chance of encountering open fractures may be higher than in the first scenario, it is not certain that the fractures in the damage zone are open and connected. Furthermore, the fault damage zone may not be so wide (Choi et al., 2016) which may mean that only a few percent of a, for instance, one kilometer horizontal well section has to accommodate the flow into- or from the reservoir. If flow and pressure communication can be achieved in this scenario, risk of induced seismicity may start to play an important part, especially for the injector well (largest effect on stress

change and fault re-activation). This should be considered before wells will be drilled (see also Buijze et al., 2019).

For both scenarios the distance between the wells will be an important consideration for development. On the one hand pressure communication between the wells is vital and wells should not be too far apart. On the other hand, early breakthrough, due to short circuits, would also result in an uneconomic project.

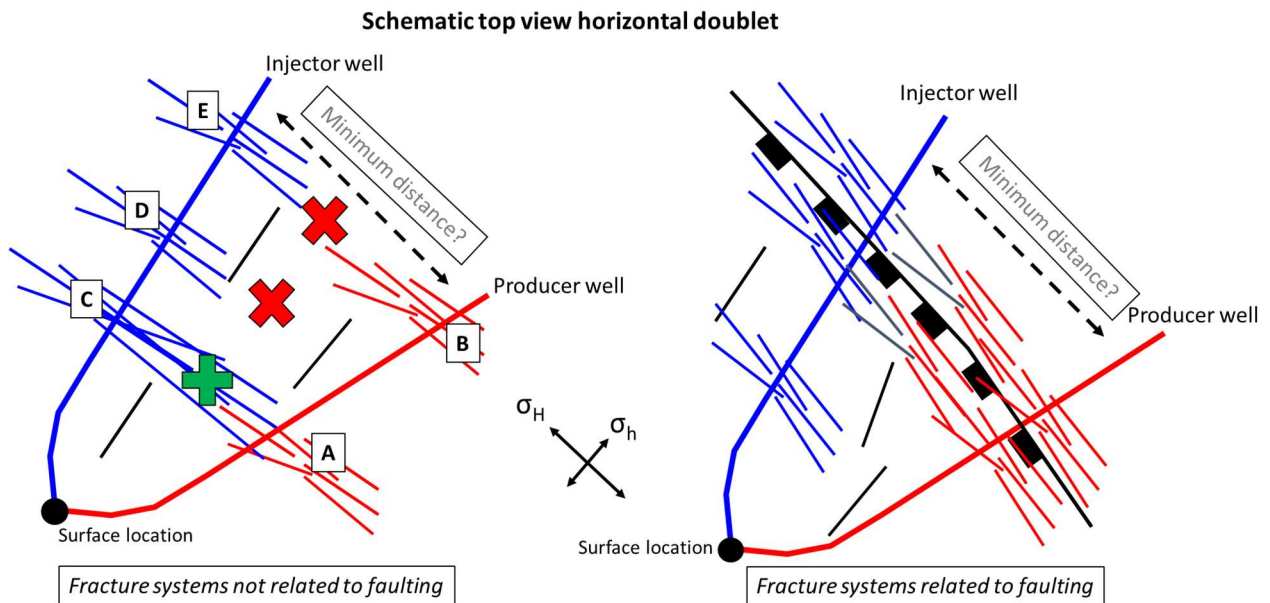


Figure 19: Schematic representation of horizontal injector - producer pair. σ_H indicating maximum horizontal stress and σ_h indicating the minimum horizontal stress. Left indicating that fracture networks encountered in one well do not necessarily connect to fracture networks encountered in the other well (A may connect to C while B, D, E are not connected). Right indicating the assumption that fractures in the fault damage zone (fault indicated in black) may potentially have a higher chance of connectivity. Early breakthrough and possible seismicity are then risks to assess in more detail.

This is one of the reasons why fractured reservoirs are often developed via grid drilling. This maximizes the chance of having sufficient flow and reducing the chance of lack of communication. Furthermore, early breakthrough may be managed by smart injection and production configurations and strategies. In case of geothermal energy the economics of such a concept may become the bottleneck.

The following considerations (among many others) play a role:

- Exploration vs immediate development – drill a pilot hole first
- Geothermal well drainage concept – drill a doublet, triplet, grid development
- Well type – vertical, slanted or horizontal well
- Aim for fractures only or also matrix porosity
- Well placement vertically within reservoir (preferred reservoir interval in case of horizontal well)
- Well placement orientation (direction in case of slanted or horizontal well)
- Well separation – minimum/maximum distance between the wells at reservoir level
- Data acquisition such as: coring, logging, pressure measurements, fluid samples
- Well testing
- Well stimulation – such as acidizing, hydraulic fracturing
- Well completion – open hole, slotted liner, cemented liner (perforated)

- Aiming for faults (permeability) vs avoiding faults (risk of seismicity, early breakthrough)
- Decision criteria for completing and drilling next well

5.7 Well type

Generally speaking, vertical wells (Figure 20) are the easiest type to drill, easiest to acquire data from and easiest to complete. They provide information on the reservoir and vertical variation within the reservoir. However, they do not provide information on horizontal variation. Vertical wells also have a much lower chance of encountering fractures as most fractures are near to vertical (Laubach, 2003). The chance is high to miss the fracture networks and thereby encountering any open fractures. This reduces the chance of being able to produce from and inject into the reservoir. It also reduces the chance of pressure and flow communication between the injector and producer to ensure circulation at economic rates.

Slanted wells typically have a deviation of 30° - 45° at reservoir level. They are more difficult to drill than a vertical well, it increases the chance of encountering fractures, but not to the extent of a horizontal well. Data acquisition and well completion could be somewhat more challenging than for a vertical well.

Horizontal wells are the most difficult ones to drill. Even when technically feasible, data acquisition will be more challenging and may be limited to certain MWD (measurement-while-drilling) tools to minimize the risk of not being able to complete the well. From a reservoir point of view it is difficult to determine in which part – vertically – of the reservoir to ‘land’ the horizontal well. Risk is that when the horizontal section lands in a section with limited number of fractures and / or limited connection to fractured beds above or below. A pilot well may in this case aid in defining the best layers to land the horizontal well. It must be noted that observing densely fractured zones vertically does not guarantee one will encounter similar quantities laterally.

For all options hydraulic (plus acid) stimulation may aid in connecting to any (open) fracture networks.

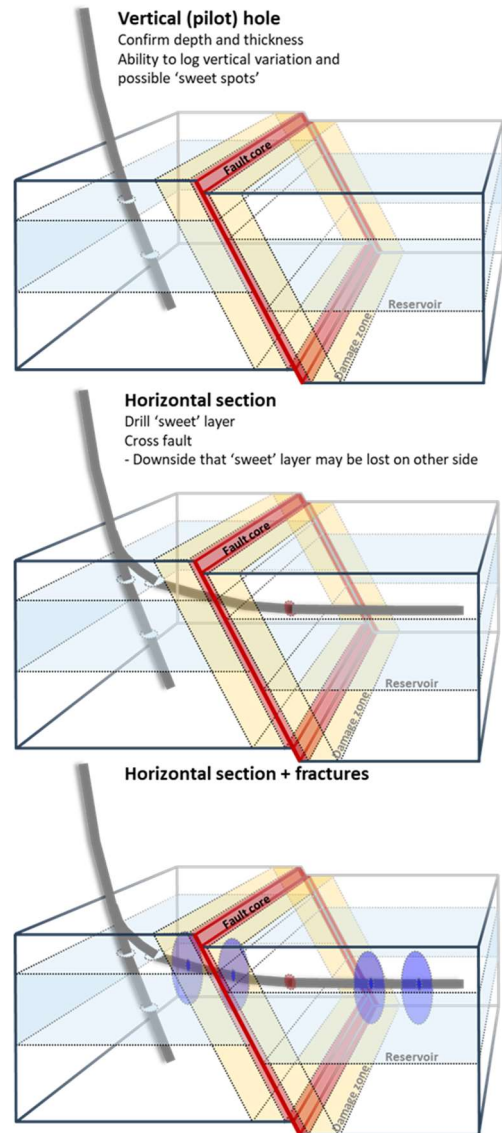


Figure 20: Schematic overview of potential development concepts.

6 Dinantian fracture observations

6.1 Observations from Dinantian outcrops and analogues

Fracture observations at surface on outcrops can be used partly as analogue for subsurface conditions in the same basin. However, caution must be taken as outcrop analogues have experienced a different geological history, have a different present day stress state and have experienced leaching (dissolution/weathering) due to meteoric water. This makes the translation from outcrop fracture densities, fracture aperture, fracture connectivity and its ability to allow flow to subsurface conditions difficult. Nevertheless, outcrop data and statistics in combination with subsurface data can still build a more complete picture of possible subsurface scenarios. This can only be done when the chosen location is representative for the population that is expected (Peacock et al, 2003). This has been successfully applied in various oil and gas projects for production as well as drilling (e.g. De Keijzer, 2007; Richard, 2015). Reith (2018) applied field observations on fault damage zones from the Hastenrath and Brees quarries into numerical flow models of the Dinantian carbonates to match the CAL-GT geothermal wells (Figure 21). Fracture density was found to decrease exponentially away from the fault.

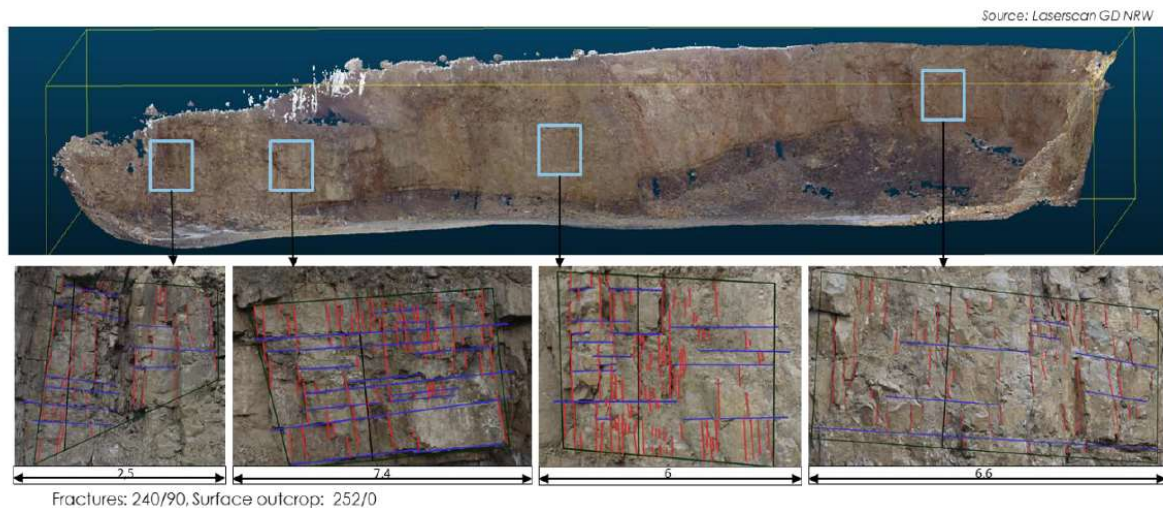


Figure 21: Fracture densities related to faults, measured on outcrop analogue by Reith (2018). (Scale in meters)

Various Dinantian outcrops can be found in Belgium which could act as outcrop analogues (Hance et al., 2006a; Hance et al, 2006b; Poty, 2016; UK (e.g. Derbyshire Peak District (Breislin, 2018)). Various other locations worldwide can further enlarge insights into similar deposits and or fracturing (e.g. Hardebol et al., 2015; Bisdorn, 2016). As subsurface analogues in The Netherlands fractured Zechstein reservoirs may be considered for extra data gathering and scaling these to Dinantian conditions.

No outcrop data were acquired in this study.

6.2 Fracture observations from seismic

Fractures cannot be observed directly from seismic data as the fractures and their displacement are well below seismic resolution (Table 4). Efforts may be made with seismic inversion to use rock mechanical properties to derive for instance (fracture) porosity. However, the depth and seismic data quality across the Dinantian may hamper efforts like these. Also, the limited number of Dinantian wells available for calibration make this type of work challenging. Seismic data, preferably 3D, may however help in detailed fault mapping and structural analysis. This work could provide valuable insights that help to highlight areas where theoretically the fracture density is largest. The reader is

also referred to the SCAN seismic interpretation report (Ten Veen et al, 2019) where seismic attributes have been used to create detailed fault interpretation.

6.3 Fracture observations from well data

Fractures in the subsurface can be identified directly by means of core and borehole image logs or deduced indirectly by drilling events (losses, gains, changes in ROP), well testing and production data, including production logging.

6.3.1 Dinantian drilling events

For drilling operations (open) fracture systems may cause serious issues with either losses, gains (in over-pressured systems), well bore stability and/or erratic rates of penetration (ROP) (e.g. bitdrops). All these issues have been experienced by wells that drilled the Dinantian carbonates in The Netherlands and are (partly) mentioned in Carlson (2019) and listed in Table 8. It is however possible that various operational issues cause some of the drilling events and that the observations have nothing to do with the geology (e.g. too high mud weight, wrong bit choice, weight on bit, poor material selection). Moreover, drilling events like losses and gains or wellbore stability are sometimes difficult to link to a specific depth. All of these can occur at depths shallower than the depth at which the bit is drilling.

6.3.2 Dinantian cores

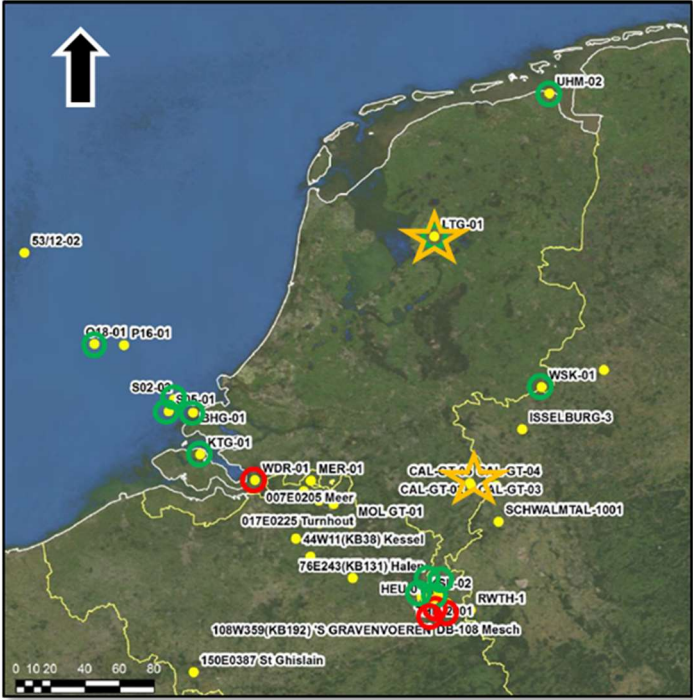
Core is a valuable information source for many geological topics (e.g. reservoir characterization). For fracture characterization it has however some limitations. This is mainly due the quick lateral and vertical variation of fracture characteristics (e.g. fracture density). In case core covers only a few percent of the total reservoir it may not provide you with information that is not representative for the entire reservoir. It does however, provide a good measure to calibrate for instance an FMI interpretation to (see LTG-01 FMI interpretation in paragraph 7.2.1). Another limitation is that the core recovery process can affect the fractures, either creating new fracture or widening pre-existing apertures (also explained in paragraph 4.2.1).

6.3.2.1 Dinantian core in The Netherlands

A total of 16 wells in The Netherlands have cores retrieved from the Dinantian carbonates (Appendix A: Data table well data). For 4 (old) wells it is not clear where or if the cores were stored and are therefore unavailable for evaluation. In all of the available cores fractures can be observed (Figure 23). In general they fall into two categories:

1. Subvertical fractures caused by tectonic and/or burial stresses
2. Subhorizontal (and possibly subvertical) brecciated fractures caused by overpressured fluids.

Figure 22: Map of The Netherlands indicating wells with core from the Dinantian (green can be visited). Wells with (also) FMI are indicated by the stars (LTG-01 in the North and CAL-GT-01-S1 South).



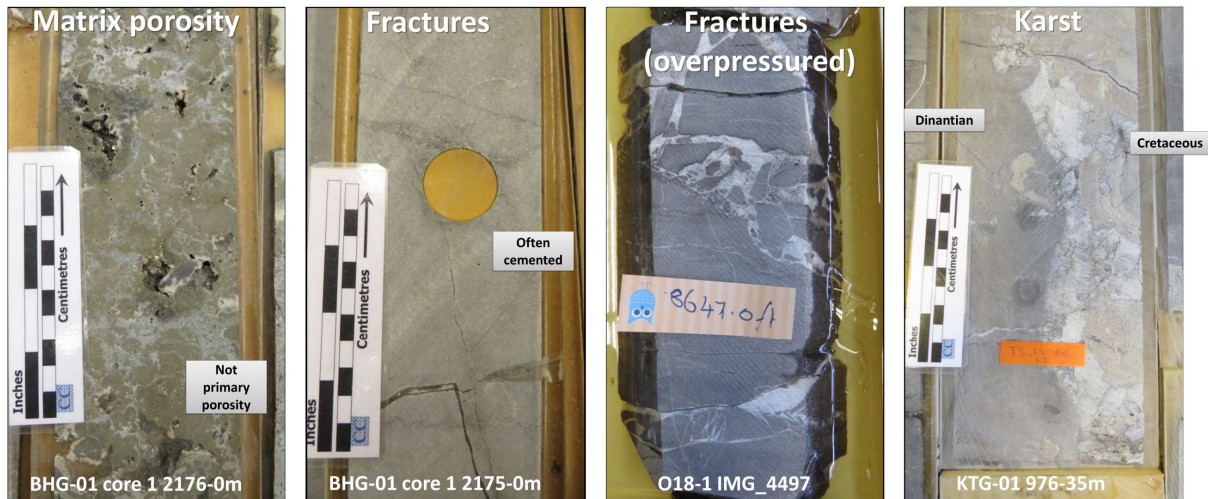


Figure 23: Examples of matrix porosity (secondary), tectonic fractures, overpressured (natural hydraulic) fractures and karst (infilled with Cretaceous sediments).

The majority of both fracture types is cemented. Occasionally, open subvertical (tectonic) fractures can be observed. It is however unclear whether these fractures existed and were open at subsurface conditions or that these are drilling/coring induced fractures or pre-existing fractures that re-opened during the process. Cemented fracture widths may be up to 2 cm.

The cored fractures would ideally tell a part of their geological history by their orientation and cements. However, none of these cores were oriented when acquired. Therefore, the azimuth will not provide reliable information on stress directions. If re-orientation could be achieved then this would still provide limited information as the main interest is in fracture density and which direction open fracture systems are oriented. As mentioned, open fractures in core have to be treated with care due to its possible relation to acquisition. No re-orientation has been attempted for this study.

6.3.2.2 Core recovery

Low core recovery could be indicative for possible open fractures and/or karst as the rock lacks cohesion making it very difficult, to recover core as being in situ. Poor recovery can however also be caused by operational problems which may have nothing to do with the cored formation. When core is poorly recovered often some or even no debris is left. Out of the 12 cored cores for 7 wells the recovery is documented. Out of these 7 wells 4 have notably poor recovery for (a part of) the cored interval (see also Table 8).

The BHG-01 well recovered 2 cores from the Dinantian and 3 from the Devonian below. One core from the Devonian (2649 – 2658m AHRT) was completely lost while the others have a 100% recovery. Wash outs also occurred in this well, but does not link up with the poorly recovered core as the wash out is located at 2413.7m (Dinantian).

The KTG-01 well encountered the Dinantian relatively shallow (945mAH) and cored three sections. All cores have 100% recovery, but losses were endured while coring which resulted in the termination of a core section prematurely. Cores show karstic sections and fractures.

The LTG-01 well has two cored intervals. 4376-4379.5 m (2.4 m recovered, 69 %); 4470-4480 m (3 m recovered, 30 %). Poor hole conditions are reported in the petrophysical report, but well below the cored interval (4775-4798mAHRT). Just below the cored interval erratic porosity is reported which may be indicative for karst. Losses while drilling have been experienced for this well. The FMI

interpretation shows faulting and possible a lot of drilling induced fractures in the upper part of the Dinantian of the LTG-01 which may partly explain the poor recovery.

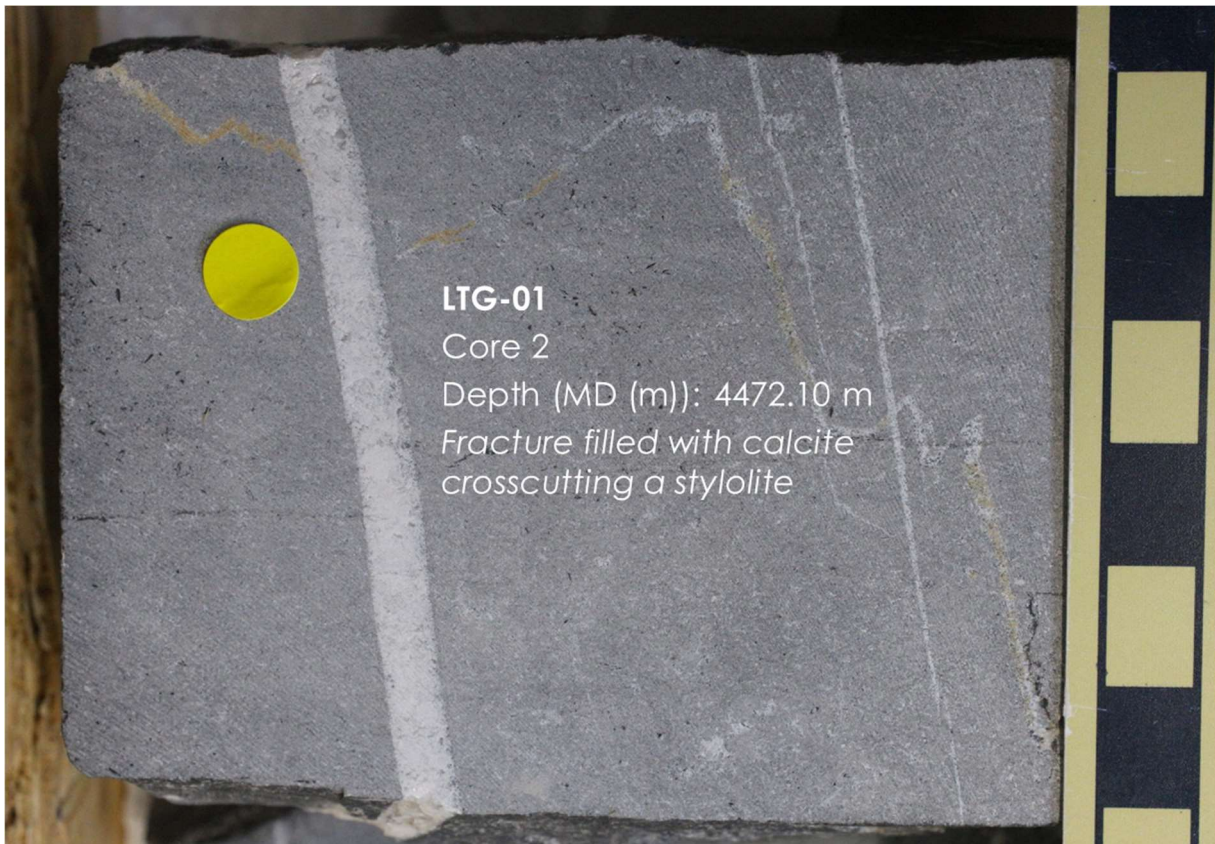


Figure 24: Part of core 2 from the LTG-01 well showing calcite filled fractures crosscutting stylolites.

The S02-02 well has 4 cores across the Dinantian and all of them show poor recovery. From 1886-1889 m, recovery 1.8 m (60 %); 1889-1898 m, recovery 5.5 m (61 %); 2417.3-2426.3 m, recovery 0.9 m (10 %), mostly rubble; 2615.8-2624.9, recovery 1.5 m (16 %); 2624.9-2633.4 m, recovered 5.9 m (70 %). In this well many wash outs as well as erratic porosity spikes have been observed by the well logs. However, no losses were reported for this well, even though it is believed that the well was drilled with up to 40 bar overbalance. In case of open fractures and/or karst losses would have been very likely.

The S05-01 well has 11 cores in the Dinantian. Only the first core had a poor recovery: from the scheduled 9 m (1190-1199 m), only 2 m was recovered. This core was taken at the top of the formation, just below the Base Cretaceous unconformity. This poor recovery is most likely related to karstification. Wash outs are reported for deeper sections.

6.3.2.3 Dinantian core DZH1 (Heibaart, Belgium)

An attempts of calibrating core observations and measurements to wellbore logs was performed on the DZH1 well by Van der Voet et al. (2019). For permeability created by joints and partially open fractures, they concluded that the distribution of joints could not be predicted, but that the development of partly open veins was strongly influenced by differential compaction. Veins were found to be more abundant in the massive boundstones than in the layered wacke- to grainstones.

6.3.3 Log observations Dinantian

Fractures and karst can affect logging as it may create wash outs or varying log responses (e.g. resulting in increased porosity evaluation). The majority of the wells that drilled the Dinantian suffered from these effect. Out of the 12 wells with cores, 8 have also wireline logs. Two wells (LTG-01 and CAL-GT-01) have borehole image logs (BHI) available. BHI's provide essential fracture information, especially when core is not oriented and the fact that this is an (indirect) measure of fractures in subsurface conditions. These BHI's (or FMI's as they were acquired by Schlumberger) have both been interpreted by the same interpreter for this study and results are listed below in this report. The other well logs indicate occasional wash outs (hole enlargements), anomalously high porosities, high Uranium values, or high bulk densities, which may be associated with fractures and/or karst. This is seen in all 12 wells (Carlson (2019) and Table 8).

6.3.4 Well test observations Dinantian wells

Well tests and pressure tests are vital data in order to assess whether the reservoir is capable to flow fluids. When this reservoir is Type I or Type II (Nelson, 2001; Figure 5) then flow is indicative for the effectiveness of the fracture system. Failed pressure tests due to inability to seal the probe to the formation may have been caused – among other reasons – by open fractures. Available well- and pressure tests are described in Carlson (2019), but also listed in this report alongside drilling events, log observations and core recovery (Table 8). The majority of the wells were targeting and testing for hydrocarbons. As most of Dinantian reservoirs that were drilled were not over-pressured (except for LTG-01 and UHM-02) the wells will likely not flow water due to the fact that the hydrostatic head will be equal to the reservoir pressure (and no ESP was used). This may bias some of the observations. Nevertheless, there are wells that do not flow at all, even despite being over-pressured (e.g. LTG-01) while others do flow with ESP (e.g. CAL-GT-01-S1 and CAL-GT-02) or could flow – possibly due to (little) overpressure (e.g. KTG-01). The (vertical) variability of the reservoir is reflected by the results of different tests on the same well. For instance, the KTG-01 well was pressure sampled by RFT's (Repeat Formation Tester) which failed as the rock was too impermeable, while the production test resulted in 369m³ of formation water in 1.5 hr.

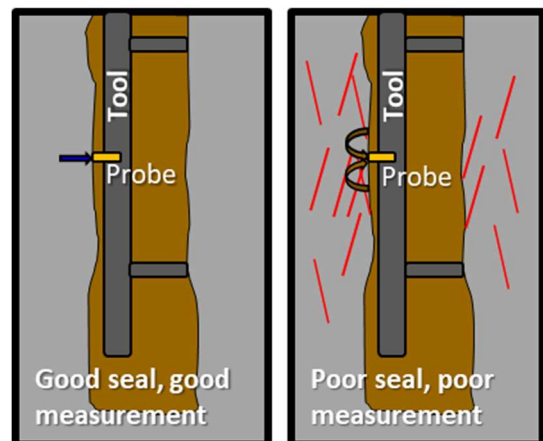


Figure 25: Sketch open borehole (brown) pressure sampling of unfractured (left) vs fractured reservoir (right). Left image indicates good sealing of the probe able to measure formation pressure and possible fluid sampling. Right image indication poor seal due to fractures, resulting in measurement of the wellbore fluid pressure.

6.3.4.1 Well productivity results Balmatt project, Mol, Belgium (MOL-GT-01/02/03)

In the Balmatt project (Mol) three wells were drilled into Dinantian limestones at 3000 – 3600m TVD and consequently tested. All targeted faulted and associated fractured intervals. It must be mentioned that interpretation is constrained by only limited seismic data therefore it may be

uncertain for some of the wells whether they actually hit similar systems. However, based on the MOL-GT-01 results it was decided to drill the MOL-GT-02 well. The latter was tested to have an injectivity index I of 1.5 – 2 m³/hr/bar which indicates relatively poor reservoir conditions (Petitclerc et al., 2017). The MOL-GT-03 well results were below expectation without any details mentioned (Broothaers et al., 2019). However, only two out of the three wells were used for production until seismicity forced the company to close in the wells and investigate its relation to the geothermal operation (EGC conference 2019).

Productivity of the Loenhout gas storage wells is not discussed as this gas storage is largely accommodated in a karstified/cave system, difficult to compare to fractured reservoir, at much shallower present day depths (~1100m TVDSS) than the Mol geothermal wells (e.g. Amantini et al., 2009).

7 FMI interpretation Dinantian wells

7.1 FMI Belgian wells

Across the Belgian border at the Balmatt project near Mol-Donk (MOL-GT wells) two more FMI interpretations were conducted independent from this project. Results have not yet been published, but some results from the MOL-GT wells which drilled likely through a fault have been presented at the European Geothermal Congress 2019 (Broothaers et al., 2019). An estimation of the aperture based on FMI may average at 170 microns (pers. comm.).

7.2 FMI LTG-01 & CAL-GT-01

The FMI's of the LTG-01 and CAL-GT-01 wells consist of oriented high-resolution, 240 trace resistivity data and were interpreted by Angela Pascerella from Panterra Geoconsultants B.V. with TerraStation software. The following features were captured in the evaluation:

- Bedding (not all beds, but enough to map general dip directions and identify faults)
- Faults
- Fractures
 - Continuous and discontinuous (partially) conductive fractures
 - Continuous and discontinuous (partially) resistive fractures
 - Faint trace fractures (very difficult to see or discontinuous)
 - As a result fracture density logs
 - As a result indication of fracture clusters (defined when fracture density is more than twice the avg fracture density of the entire interval in the specific well)
- Drilling induced fractures
- Breakouts
- Textural aspects (vugs, breccia, wash outs)

The *partially conductive/resistive fractures* class means that the sine wave of the fracture (i.e. the representation of the fracture along the borehole when projected onto a 2D plane) cannot be traced across every pad of the FMI tool. This class contains fractures that are not conductive or resistive throughout the sine wave as well as fractures that terminate at bed boundaries.

Where possible/available the FMI interpretation was accompanied by available and corrected well logs and porosity interpretations from the SCAN Dinantian petrophysical evaluation work (Carlson, 2019).

Results (listed in Table 9 of Appendix C: Table of data files shared via www.nlog.nl/scan) can be found as interpretation panels (PDF format) and data tables in text format via www.nlog.nl/scan.

7.2.1 FMI evaluation LTG-01

The LTG-01 well was drilled in 2004 by Total. Its purpose was to evaluate the Dinantian carbonates for the presence of hydrocarbons. The reservoir was found to be overpressured as expected. The overbalance in mud weight resulted in various losses. The well was tested across 4580 – 4620mAH (see Figure 47), but without indications of flow. Based on this well test and on wireline log evaluation it was concluded that no hydrocarbon accumulation was present. As part of the data acquisition across the Dinantian an FMI log was run. The FMI consists of two runs across the interval 4315 – 5165m AH (Figure 36). It covers the basal Namurian, the entire underlying Dinantian carbonate section, and the top of the Devonian below. The quality is reasonable, but poorer when compared to the CAL-GT-01 FMI.

Bedding dip azimuth points on average to the North (varying between NW and NE) with dip angles mainly below 15° and the majority of the dip between 5 and 15° (Figure 26 and Figure 27). Steeper bedding dips are most likely associated to the presence of faults. Some of the bed boundaries have a stylolitic appearance. These were not classified as stylolites, but used as bed boundaries instead. Between 4355 – 4468m AH it was difficult to differentiate bedding planes. (see also *Drilling induced features* below)

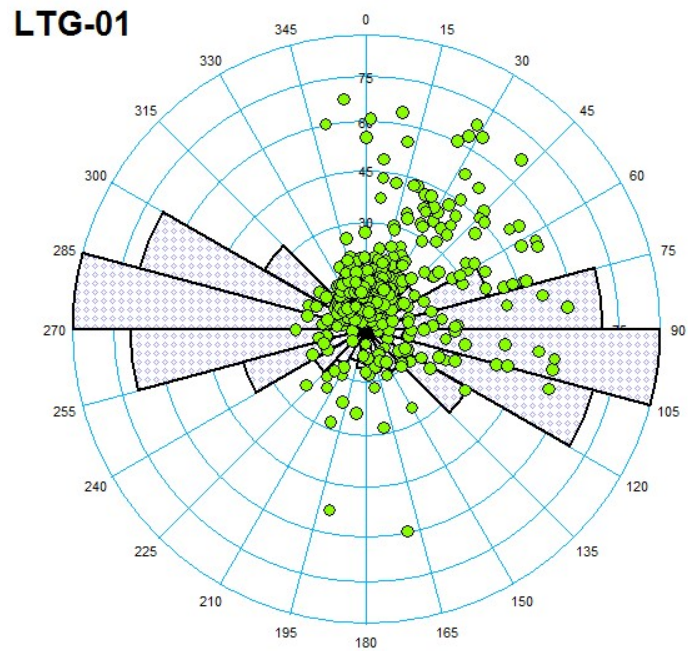


Figure 26: Bedding strike orientation (filled quadrants), dip and azimuth (points) of LTG-01.

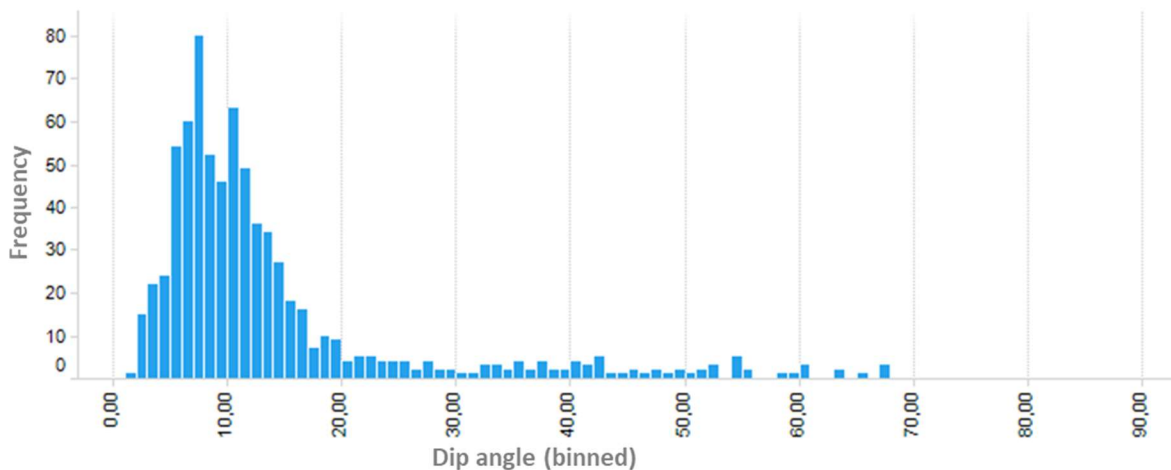


Figure 27: Bedding dip and azimuth of the LTG-01 Dinantian strata. High angle bed dipping angles are likely caused by faulting.

Six **faults** were interpreted within the Dinantian interval (e.g. Figure 30), half of them being continuous conductive and the other half partially conductive (Figure 28). The faults at the base Dinantian seem to be part of a more faulted/ fractured zone extending into or originating from the Devonian below. Faults strike varies for the various faults with orientations ranging between NW-SE or NE-SW. Fault dips vary between 41 and 89 degrees.

LTG-01

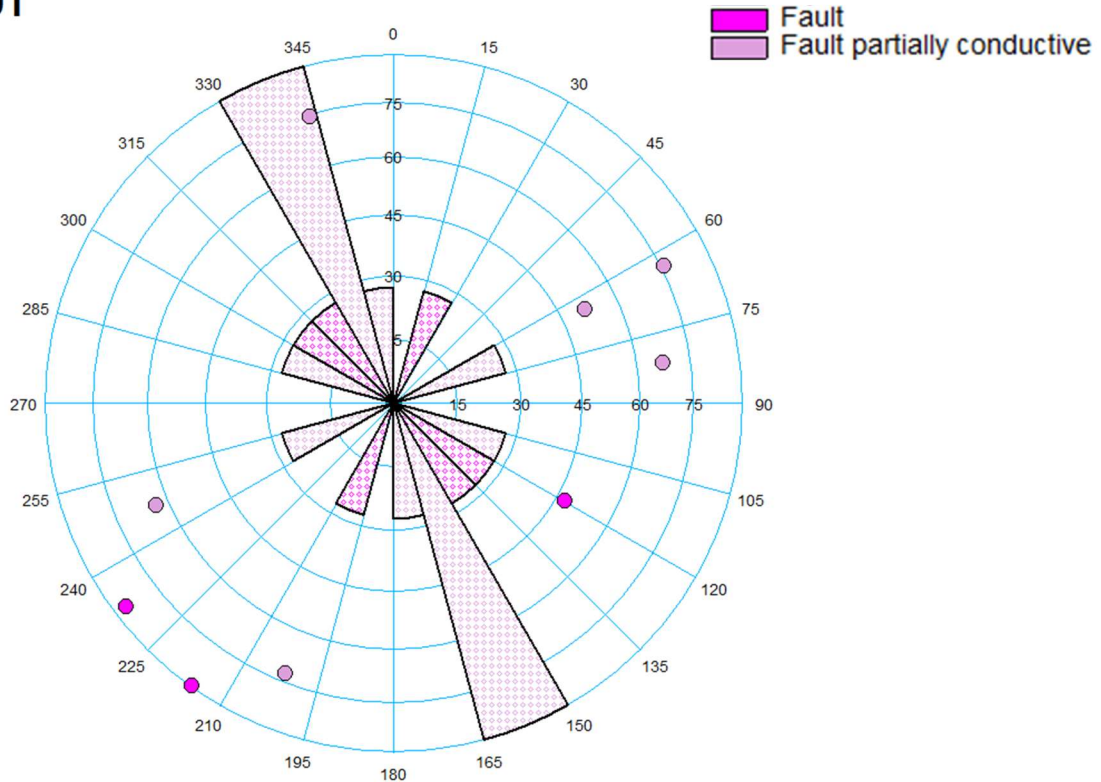


Figure 28: Fault strike orientation (filled quadrants), dip and azimuth (points) of LTG-01.

Fractures are abundant in the Dinantian of the LTG-01 well adding up 915 in total, averaging at 1.2 fractures/m when the 5 fracture classes are combined. Within densely fractured zones density reaches up to ~ 5 fractures/m (all fractures combined; Table 5). The majority of these fractures strike NW-SE (Figure 29). Fracture dip angles are high with the majority dipping $>60^\circ$.

A total of 595 *partially continuous conductive* fractures have been interpreted. The discontinuous fractures are fractures that cannot be traced on all of the pads of the borehole image tool. Also fractures that are bed bounded (truncated) and therefore not interpreted as a complete sine wave belong to this class. *Continuous conductive* (likely open) fractures are observed but are limited to 31 in total within the Dinantian. These fracture densities show peaks of max 2 fractures/m. The fractures' strikes are in line with the overall orientation, mainly NW-SE (see Figure 29 and Figure 32) and are near vertical ($>75^\circ$). Conductive fractures may be an indication of having open fractures. However, the Dinantian was drilled overbalanced. It cannot be excluded that pre-existing fractures were opened by the overbalanced mud weight. Remarkably, no resistive fractures could be interpreted.

Fracture clusters have been defined for the LTG-01 well when the fracture density exceeds 3/m. A cluster 4650 – 4660mMD may be related to an identified fault above. Multiple clusters can also be identified near the base of the Dinantian which is also more faulted.

LTG-01

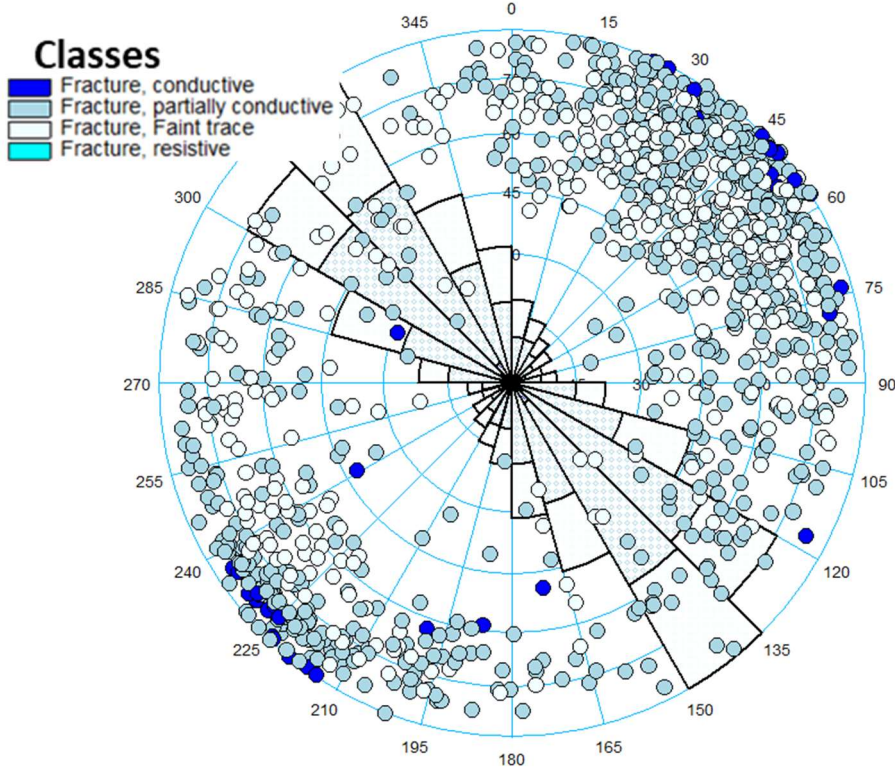


Figure 29: Conductive and partly conductive fracture strike orientation (filled quadrants), dip and azimuth (points) of LTG-01.

Table 5: Fracture observations from FMI in LTG-01.

Type	Count
Fracture conductive (no shear)	31
Fracture partially conductive (no shear)	595
Fracture partially resistive (no shear)	1
Fault conductive	3
Fault partially conductive	3
Faint Trace Fracture (no shear)	288
Total fracs	915
Average fractures	1,2

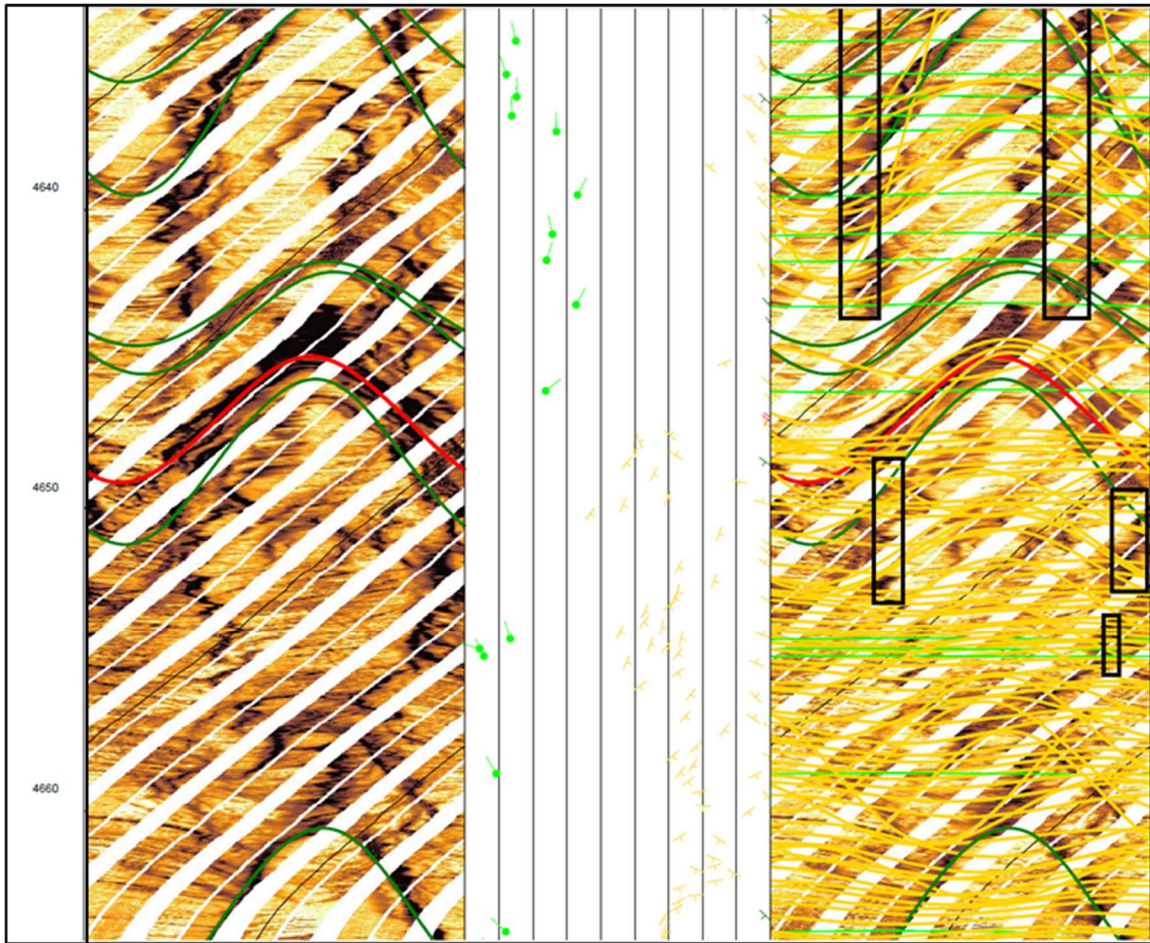


Figure 30: Example of fault (red), continuous conductive fracture (green) and partially continuous conductive fractures (yellow) in LTG-01. (FMI shown in a static color panel (left) and dynamic color panel (right). Dark colors indicate high conductivity and lighter colors high resistivity)

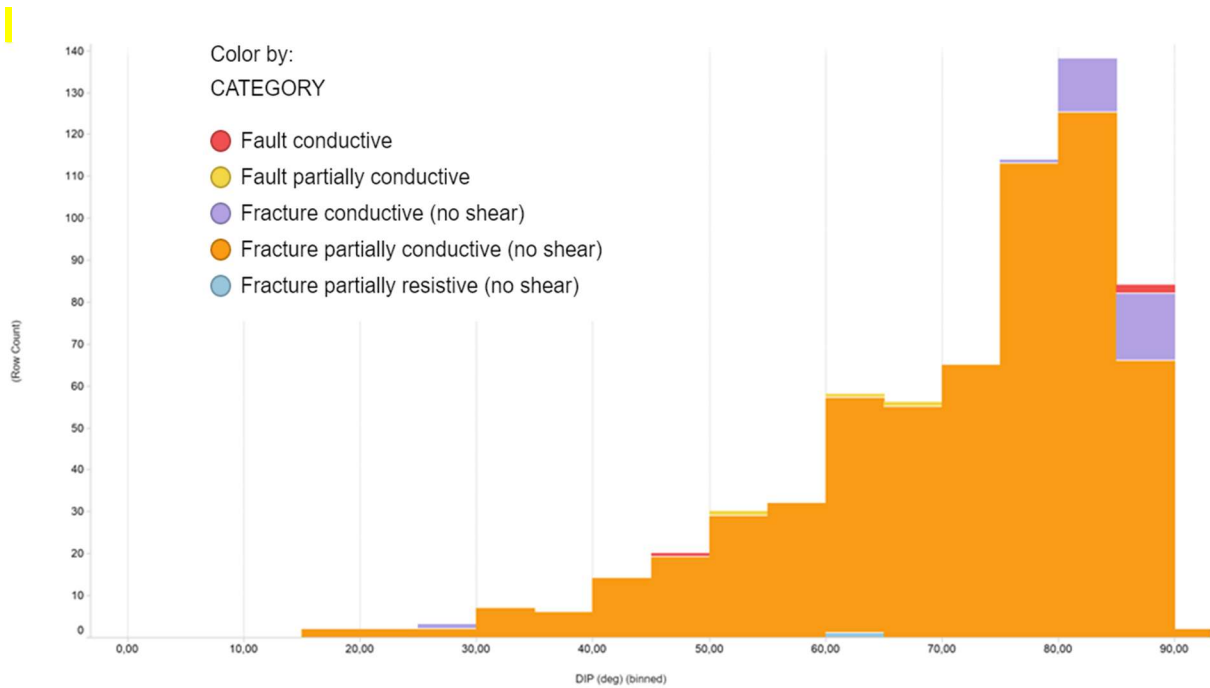


Figure 31: Fracture and fault dip angles in LTG-01. Fracture dip is pre-dominantly sub-vertical. The faint trace class has been left out of this figure.

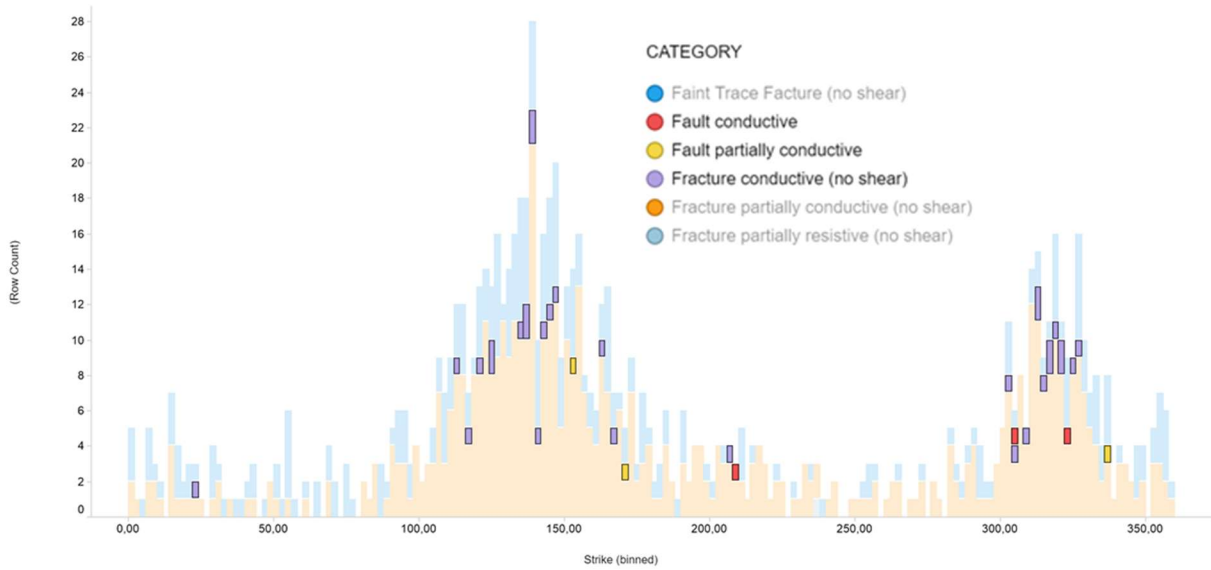


Figure 32: Orientation (strike) of conductive faults and fractures in LTG-01. Plot shows that they are mainly SE – NW oriented. Highlighted are the conductive

Drilling induced fractures (Figure 33, Figure 34) are seen throughout the Dinantian section which could be expected as the well was drilled heavily overbalanced and sustained multiple mudlosses and gains. The drilling induced fractures or tensile fracture strike is parallel to the present day stress field orientation (maximum horizontal stress). The induced fractures are predominantly oriented NW-SE. From the top of the Dinantian (4355m AH) down to a fault interpreted at 4506mAH it was difficult to interpret. First pass interpretation hinted towards vertical bedding. However, a closer look at core indicated horizontal bedding. Therefore, interpreted feature across this interval were classified as *unclear*. This vertical features may be drilling induced fractures in a high resistive matrix with hardly any bedding contrast.

LTG-01

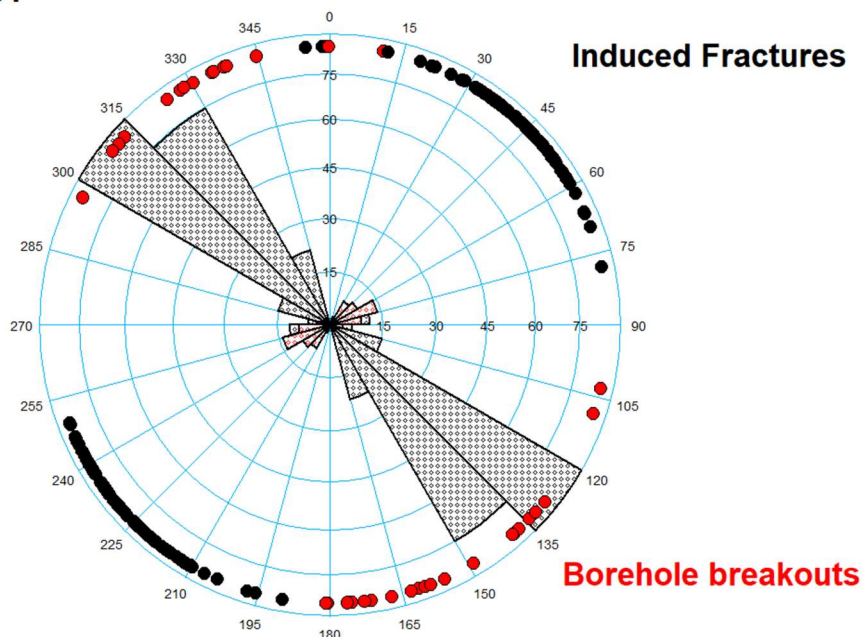


Figure 33: Drilling-induced fractures and borehole breakouts strike orientation (filled quadrants), dip and azimuth (points) of LTG-01.

Borehole break outs (Figure 33) are also interpreted and indicate the direction of the minimum horizontal stress. Theoretically this would be perpendicular to the tensile fractures, but seem more NEE-SWW oriented (slightly rotated w.r.t. tensile fractures, not exactly perpendicular). It should be noted that breakout recognition and orientation is much more uncertain than the tensile fracture characterization as the tensile fracture are much better defined on the FMI.

(PLEASE NOTE THAT THE FMI INTERPRETATION PANELS THAT ARE ALSO PUBLISHED VIA WWW.NLOG.NL/SCAN INDICATE THE AZIMUTH OF THE INDUCED FRACTURES AND BREAKOUT AND NOT THE STRIKE LIKE FOR THE FRACS AND BEDDING!)

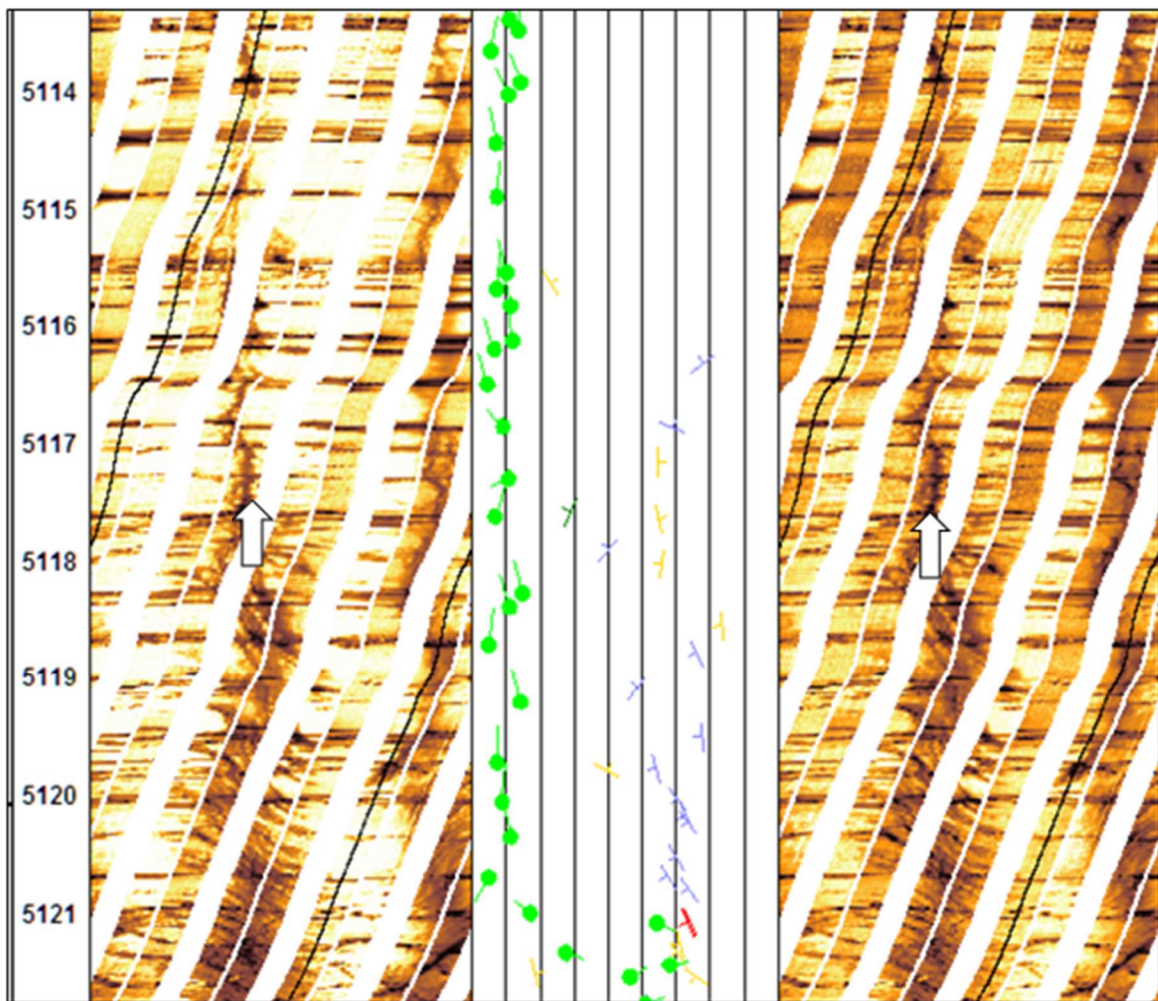


Figure 34: Example of tensile fractures (drilling induced fractures) indicated by the white arrows in LTG-01. (FMI shown in a static color panel (left) and dynamic color panel (right). Dark colors indicate high conductivity and lighter colors high resistivity)

Textural observations were made when obvious. No special in depth analysis was done on this. **Vugs** are recognized in the lower part of the Dinantian (see Figure 35). This observation coincides with a more dolomitic section with higher porosity. Vugs show as very conductive 'spots' these could theoretically also be caused by pyrite. In this case the correlation with the porosity log does point more towards real vugs. Moreover, pyrite was observed in the cores, but not as nodules. A **brecciated** area is recognized at the very base of the carbonate, just above the Devonian. This breccia could be depositional, associated to faulting or even collapsed karst. A major **wash out** around 4780mAH caused very poor FMI quality.

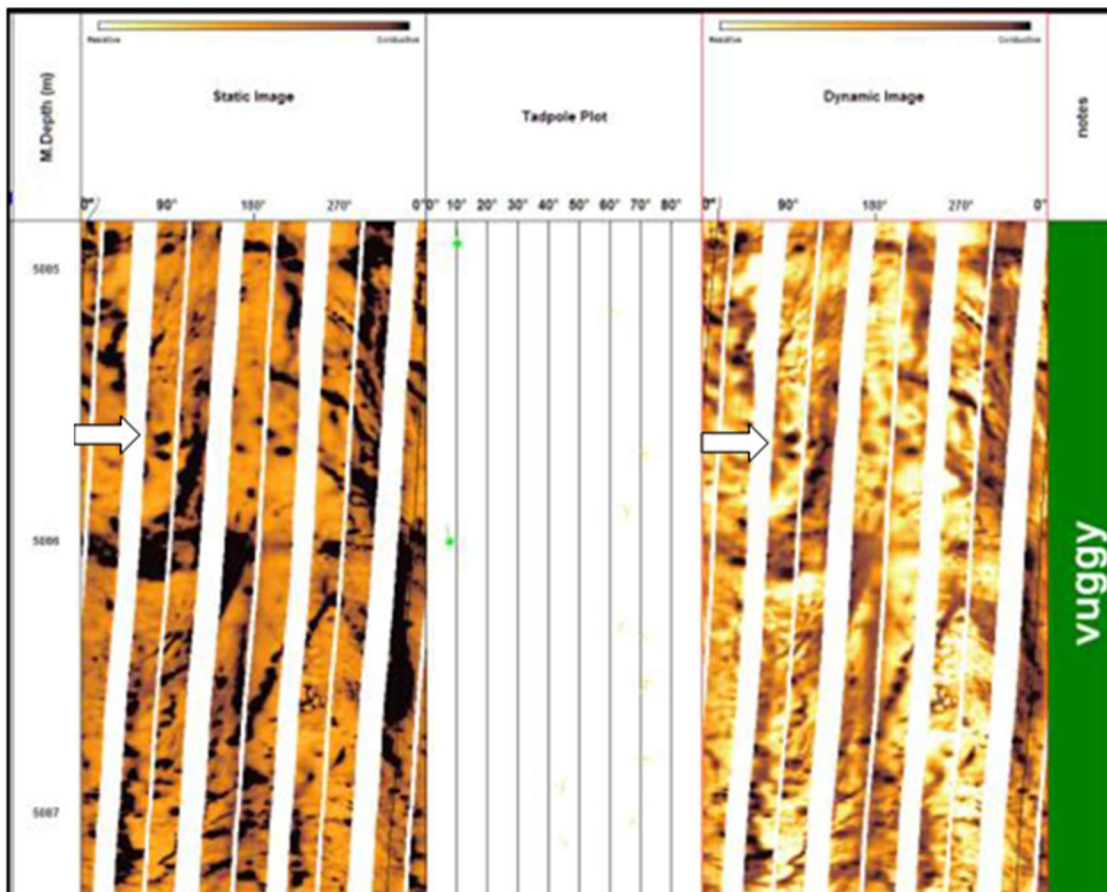


Figure 35: Example of vuggy porosity in LTG-01. Note the dark spots, also indicated with white arrows in the FMI panel. (FMI shown in a static color panel (left) and dynamic color panel (right). Dark colors indicate high conductivity and lighter colors high resistivity)

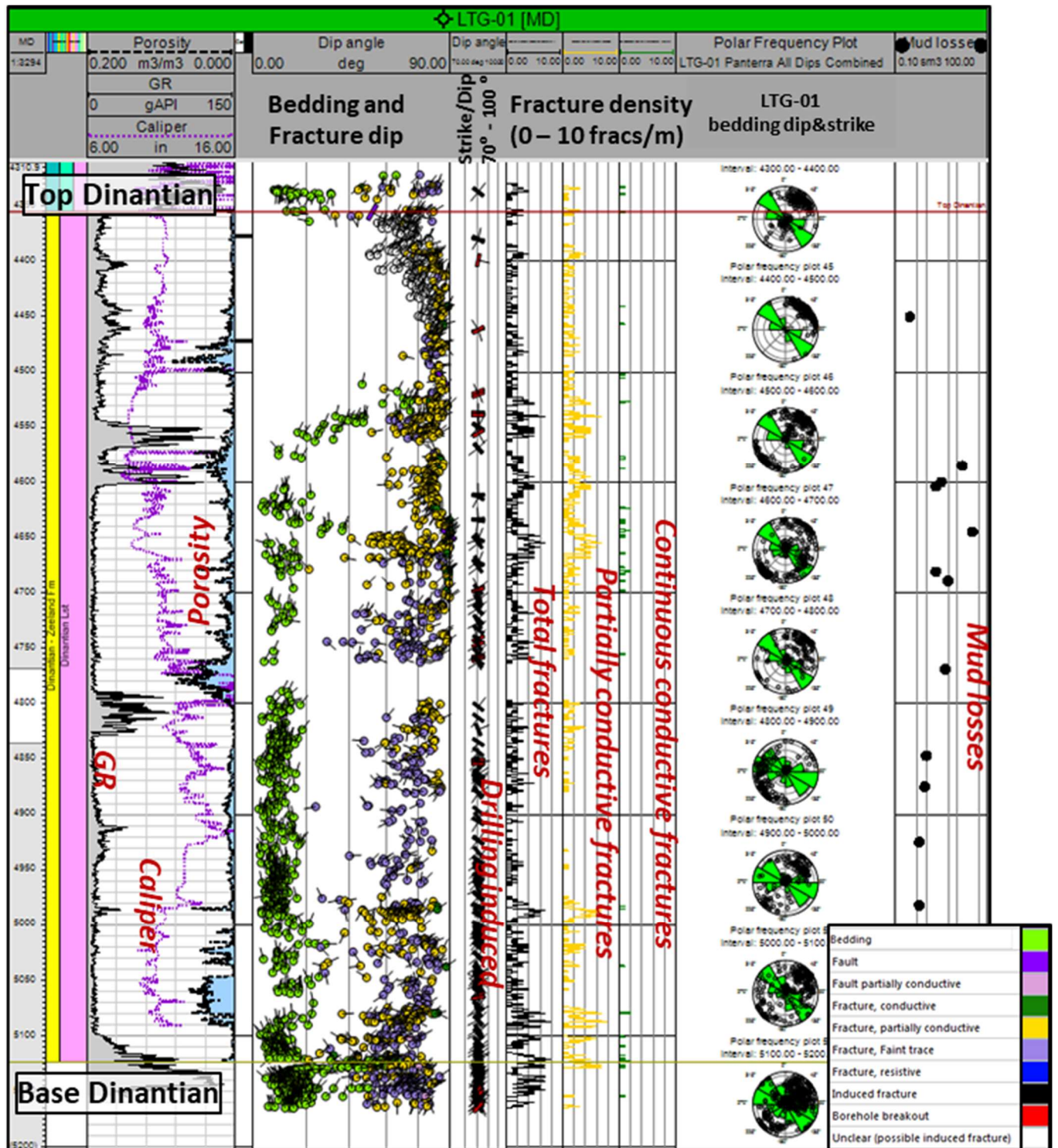


Figure 36: Well panel of LTG-01 logs and interpretations. GR, caliper and porosity are displayed in the left outer track. Next to that results from the FMI interpretation are presented in a tadpole track; bedding (green), partially conductive fractures (yellow), faint trace (purple). Dip angle of drilling induced features striking mainly NW-SE. Interpretation panels are published via www.nlog.nl/scan.

7.2.2 FMI evaluation CAL-GT-01

The CAL-GT-01 well was drilled in 2012 by Californië Wijnen Geothermie BV. The well was targeted at the Dinantian carbonates. The well hit a likely karstified interval in the Dinantian causing total losses and making logging difficult. Eventually, the karst also resulted in a sidetrack CAL-GT-01-S1 as the original hole could not be found after a check trip across the loss zone (likely karstified section). This well was successfully completed as part of a geothermal triplet development. As part of the data acquisition an FMI log was acquired, funded by EBN. The FMI consists of a single run from ~1580 – 1760mAH (Figure 46). It covers a few meters of the basal Namurian and the top of the underlying Dinantian carbonates. A large karst/cave starting around 1738mAH resulted in a poor FMI making the last 22m unusable. This interval also correlates to reported losses. A cave deeper in the section was the cause of the eventual loss of this wellbore after which it was sidetracked (CAL-GT-S1).

The FMI of CAL-GT-01 shows well stratified **bedding**. Bedding dip azimuth points to a WSW direction with dip angles mainly between 15 and 35 degrees (Figure 37 and Figure 38). Changes in bedding dip could be caused by faulting as the well is drilled into a fault zone and also the FMI shows many (minor) faults. A fault was observed around 2330mAH, but this is below the logged FMI interval. Bed dip azimuth are however very consistent and depositional effects on the bedding dip cannot be ruled out.

Figure 37: Bedding strike orientation (filled quadrants), dip and azimuth (points) of CAL-GT-01.

CAL-GT-01

■ Bedding

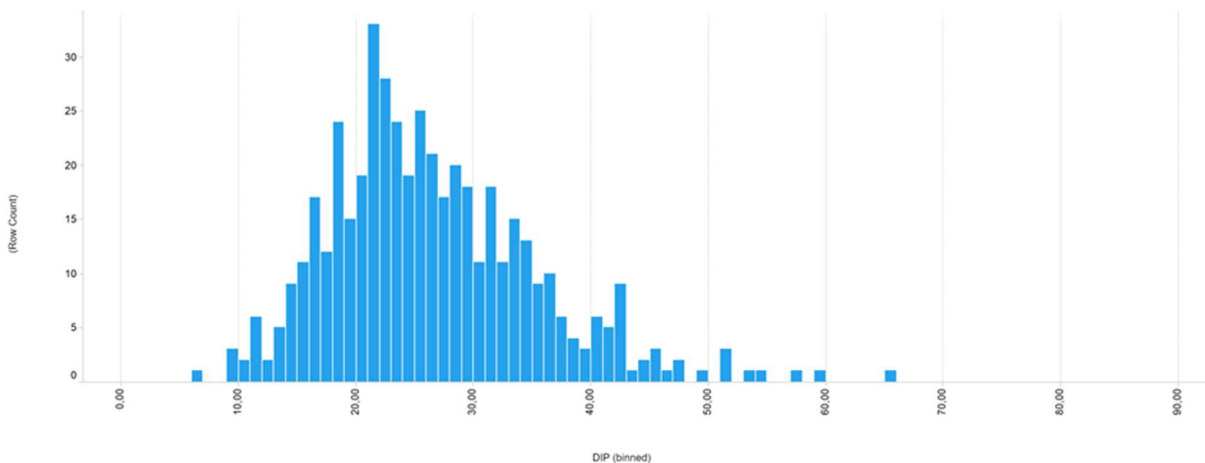
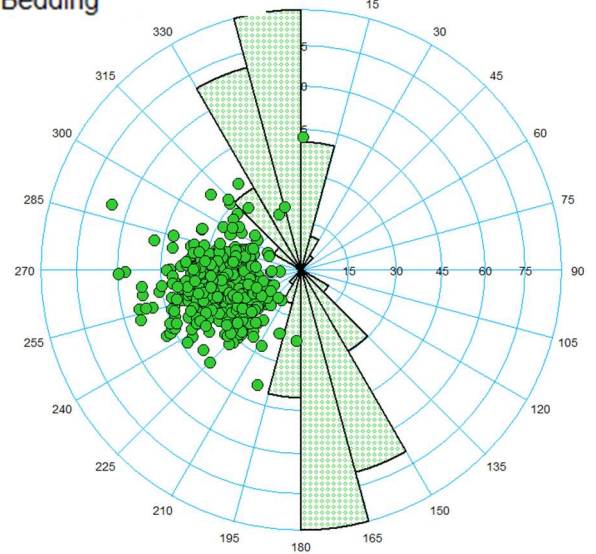


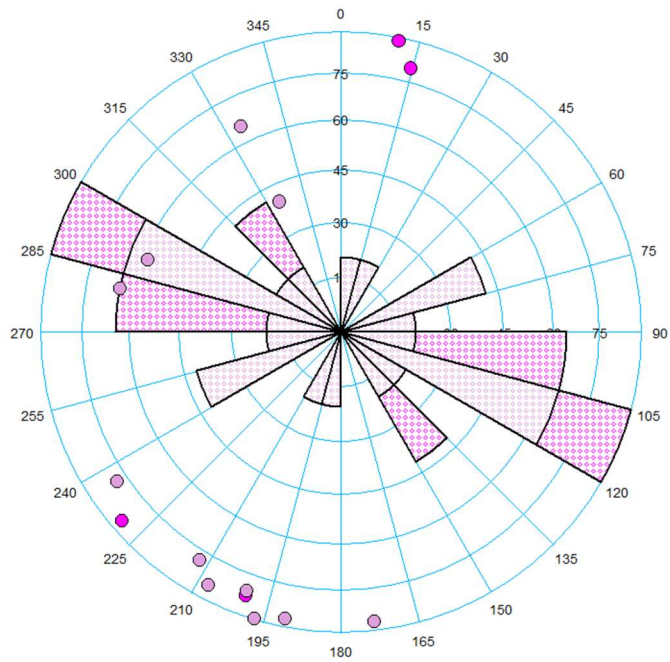
Figure 38: Bed dips and dip azimuth indicating WNW orientation with dips mainly between 15 and 35 degrees.

CAL-GT-01

Figure 39: Fault strike orientation (filled quadrants), dip and azimuth (points) of CAL-GT-01.

A total of 13 faults have been interpreted based on dip angle changes and offsets seen on the FMI. 3 of these faults are continuous conductive and the other only partially. Fault strikes vary considerably but can be roughly split into WNW and NNE groups. Some of the faults show only minor displacement.

The Dinantian in CAL-GT-01 contains many fractures adding up to a total of 431 resulting in an average of 3 fractures per meter (Table 6). Only 10 fractures are continuous conductive while 199



partially conductive fractures were interpreted from the FMI log. Total fracture density can occasionally reach 10 fractures per meter. The continuous conductive fractures and faults show spikes up to 2-3 fractures/faults per meter for the specific intervals and are mainly subvertical ($>70^\circ$). Some fractures are noted to end at bed boundaries (<5 interpreted). Fracture clusters are defined when conductive (continuous and discontinuous) fracture density exceeds 6 fractures per meter. These clusters start at 1660mAH until the base of the FMI log. Fractures are mainly oriented WNW and dip steeply ($>60^\circ$) toward the North and South (Figure 41, Figure 42 and Figure 43). The fracture orientation is different from the Tegelen fault orientation which is NNW-SSE.

Table 6: Overview of number of interpreted natural fault and fracture features in CAL-GT-01.

Type Count	
Fracture conductive (no shear)	10
Fracture partially conductive (no shear)	199
Fracture partially resistive (no shear)	38
Fracture resistive (no shear)	5
Fault conductive	3
Fault partially conductive	10
Faint Trace Fracture (shear)	2
Faint Trace Fracture (no shear)	177
Total fracs	431
Average fractures	3,0

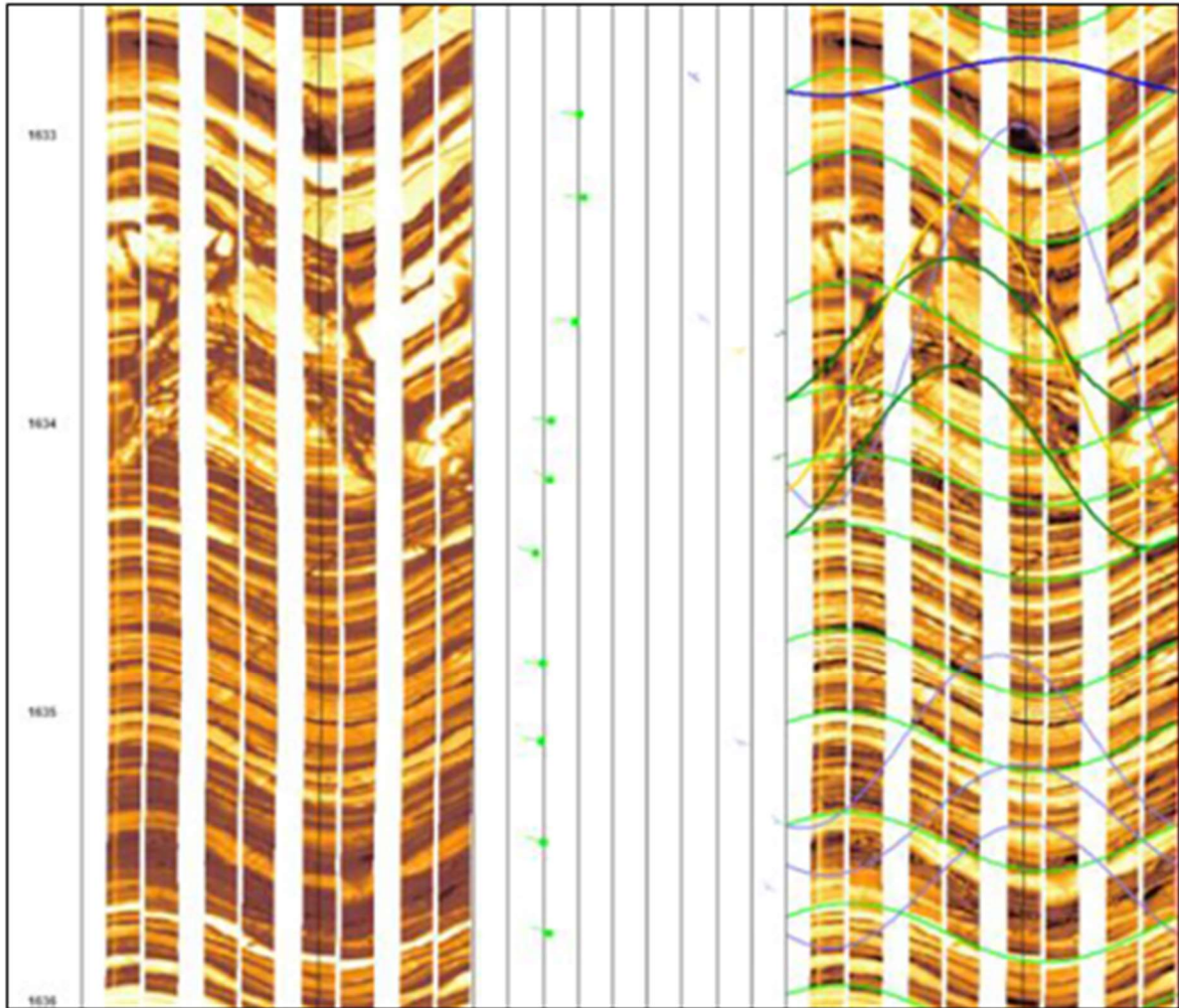


Figure 40: Example of natural conductive fractures between 1633-1634mAH. (FMI shown in a static color panel (left) and dynamic color panel (right). Dark colors indicate high conductivity and lighter colors high resistivity. The sinuses are interpretations of different features like: bedding planes (light green), conductive fractures (dark green), partially conductive fractures (orange), faint trace fractures (purple).

CAL-GT-01

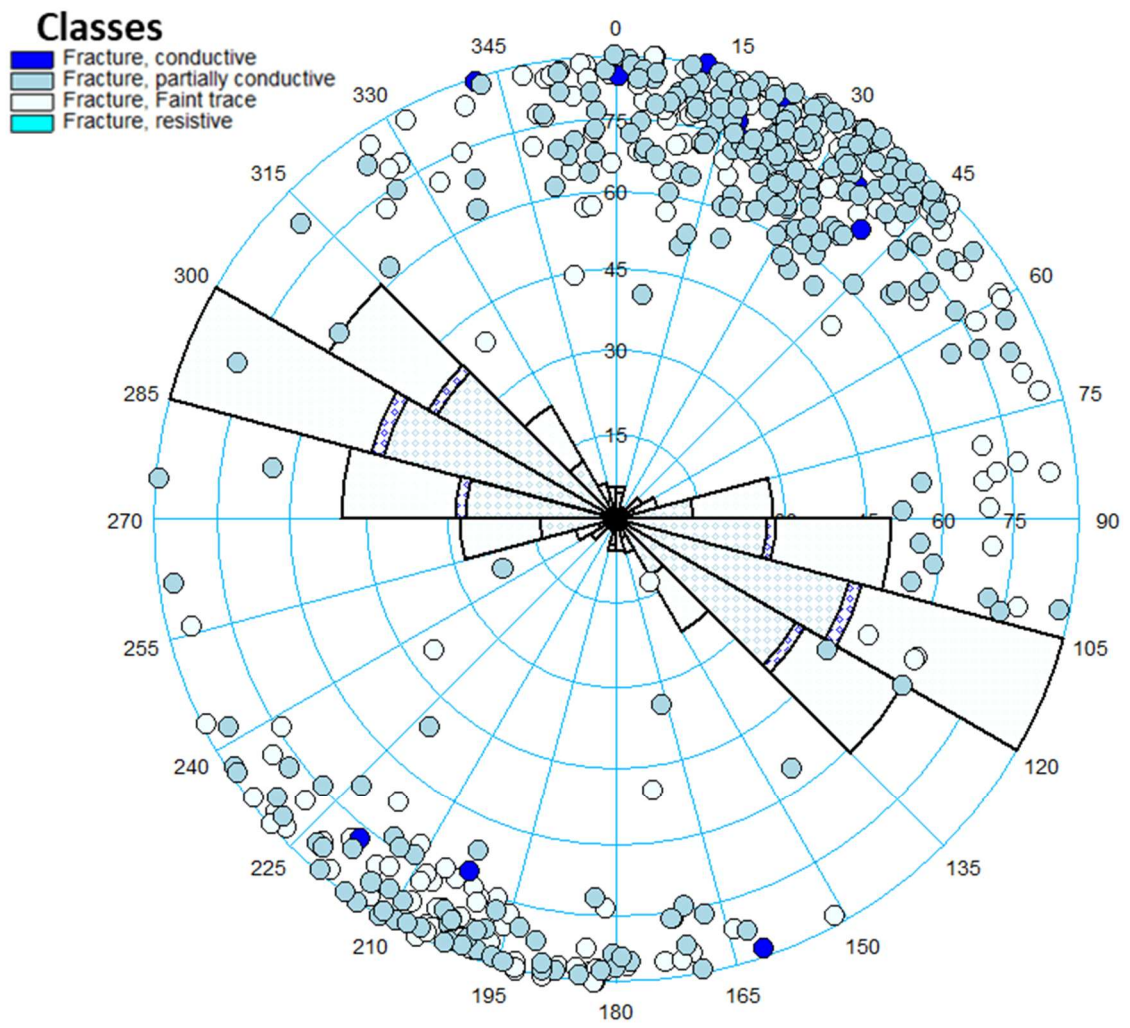


Figure 41: Fracture strike orientation (filled quadrants), dip and azimuth (points) of CAL-GT-01.

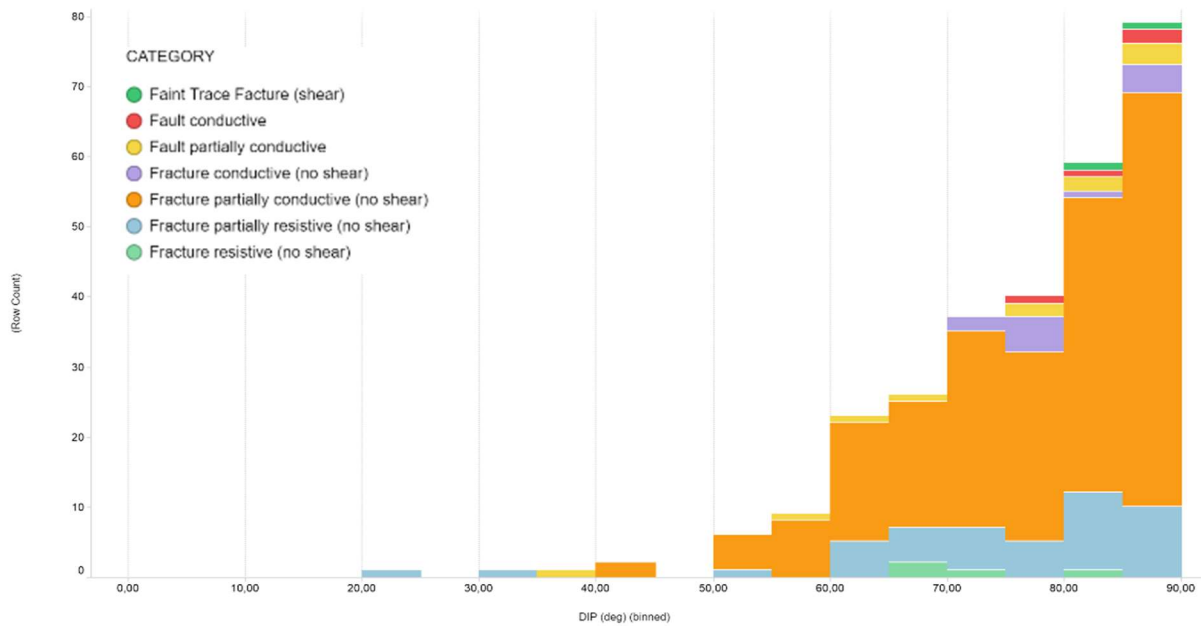


Figure 42: Natural fracture and fault orientation and dips. The stereonet shows strike with the filled quadrants and dip azimuth with points. (please note that total number vary slightly from Table 1 as this plot does not reflect the ‘faint trace’ class

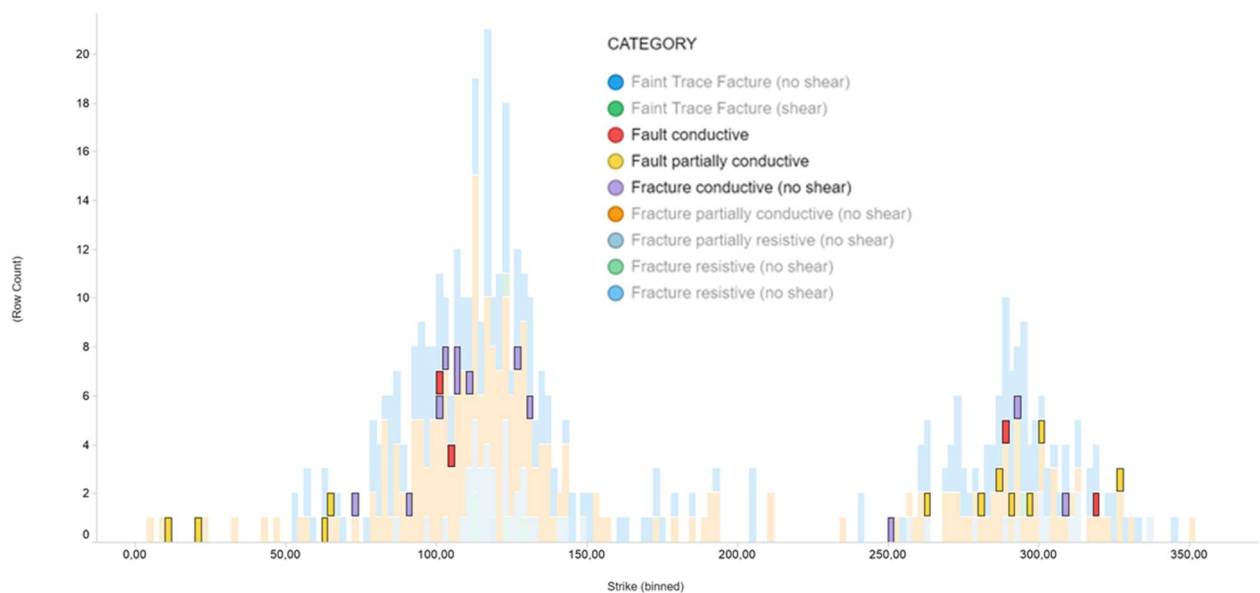


Figure 43: Histogram showing the fracture strike orientation for the CAL-GT-01 well. Plot shows that they are mainly ESE-WNW oriented. Fault and fully conductive fractures are highlighted showing that are similar oriented as the majority of the fractures and faults.

Drilling induced fractures were not easily recognized. This has most likely to do with the drilling procedures as the well was drilled with no or little overbalance. Five induced fractures could be recognized which show a NW-SE strike direction (Figure 44).

Break outs were not identified.

Textural features consist out of 4 intervals of vuggy porosity. These vugs are not necessarily related to fractures, but could be indications of karstification. Also depositional, lithological related effects cannot be ruled out.

CAL-GT-01

■ Induced fracture

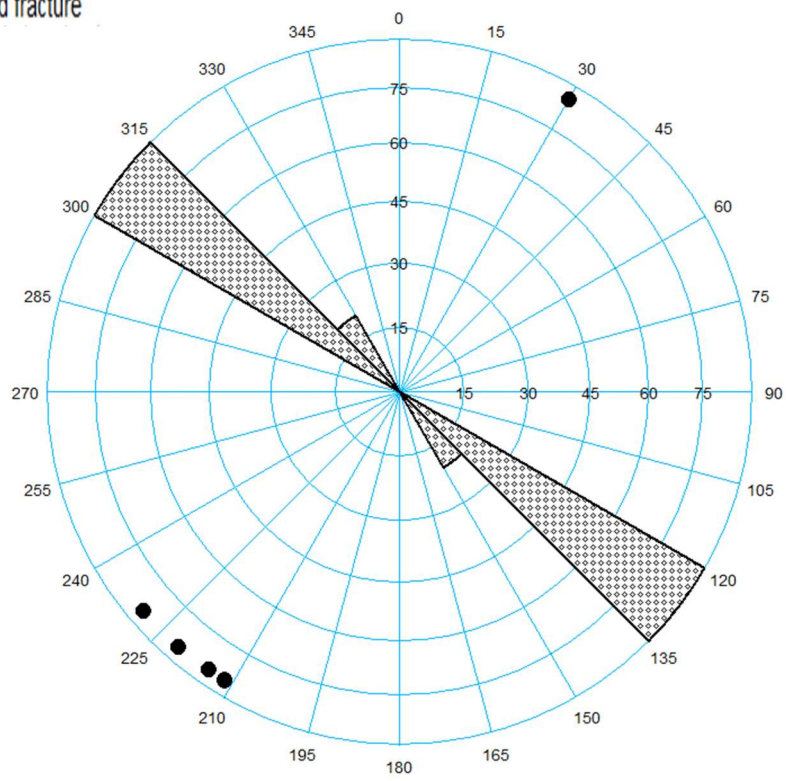


Figure 44: Drilling-induced fractures strike orientation (filled quadrants), dip and azimuth (points) of CAL-GT-01.

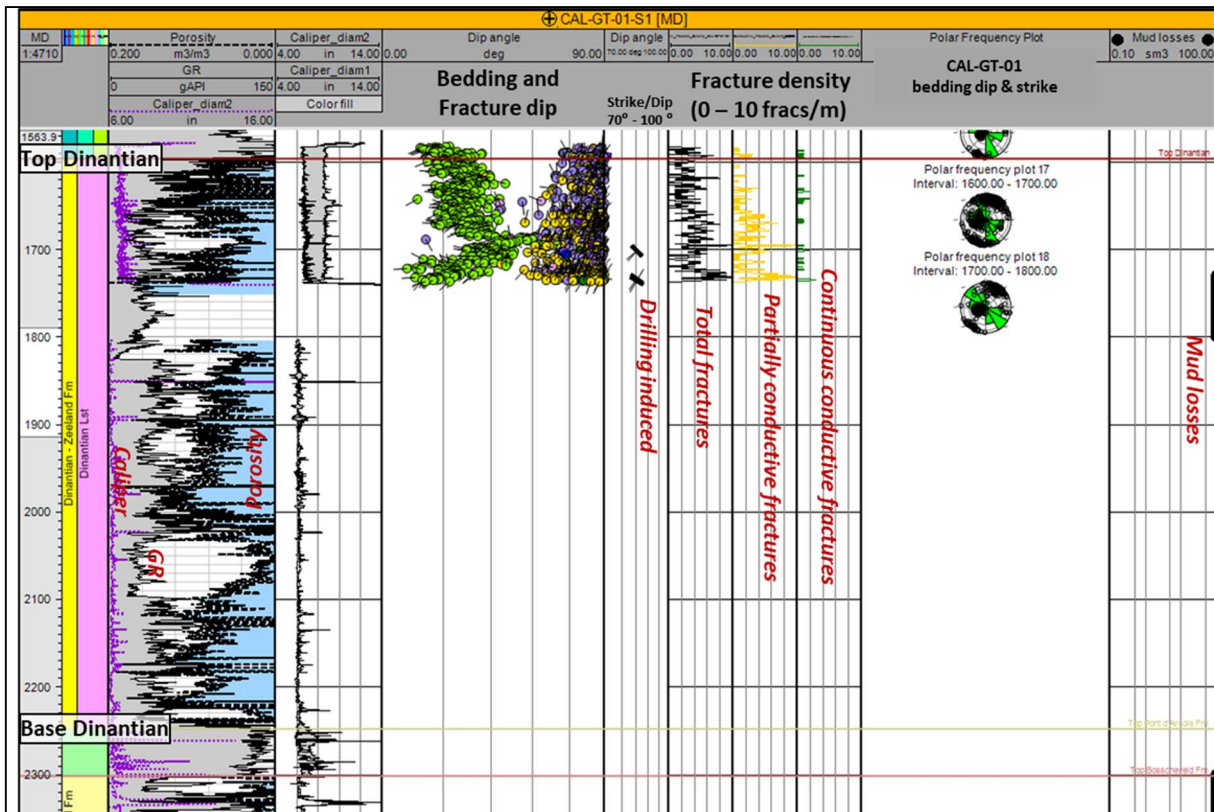


Figure 46: Well panel of CAL-GT-01 and interpretations (from Carlson, 2019) and results from the the FMI interpretation. bedding (green), partially conductive fractures (yellow), faint trace (purple). Dip angle of drilling induced features striking mainly NW-SE.

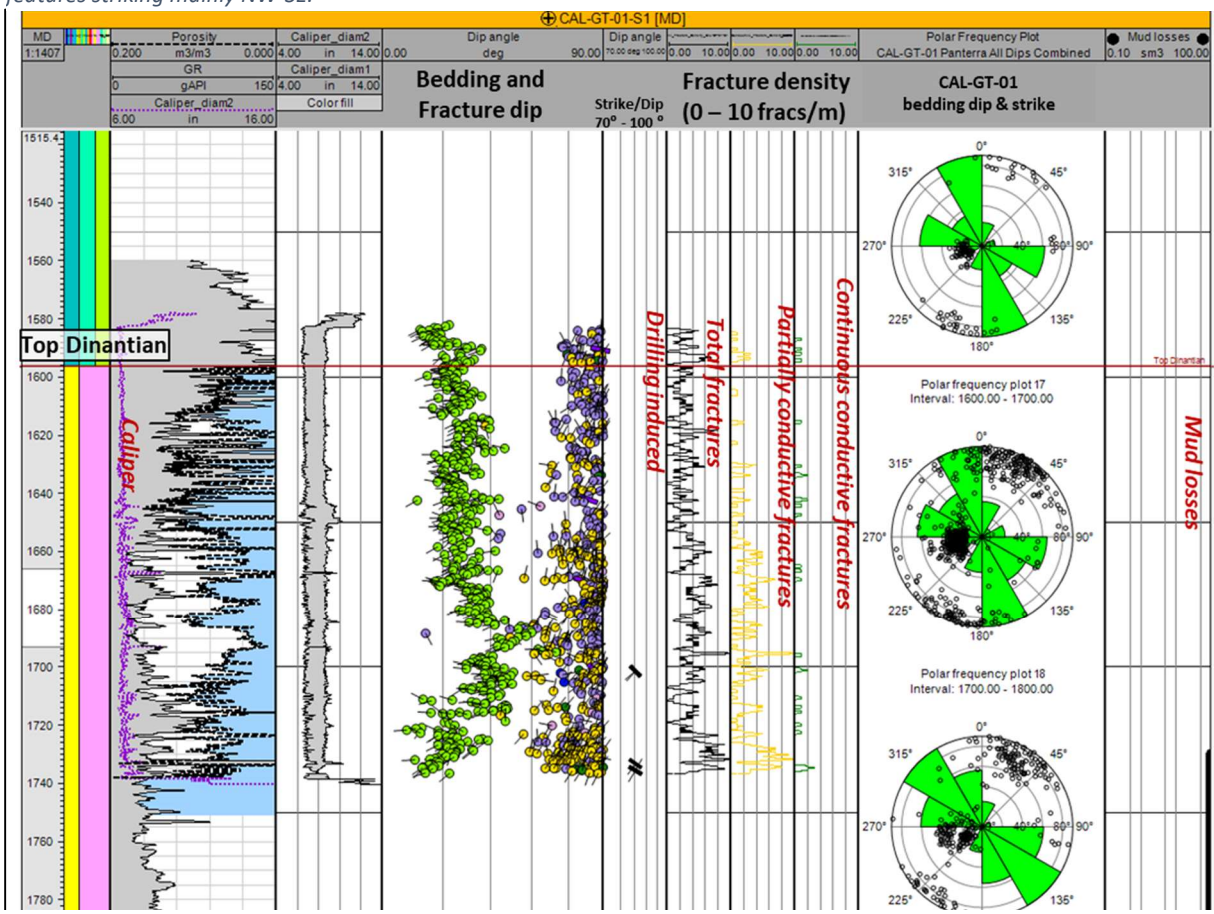


Figure 45: Focus on Dinantian section of CAL-GT-01-S1 that was logged by FMI.

7.2.3 Discussion FMI interpretations

By analysing the FMI's of the LTG-01 and CAL-GT-01 wells one has to be aware that these represent Dinantian carbonates at two completely different settings.

LTG-01 explored for hydrocarbon presence and was drilled into a – possibly distal – isolated platform (basinal structural high (Mozafari et al., 2019)), deeply buried beneath Namurian mudstones and younger strata adding up to more than 4 km. The well was drilled heavily overbalanced to withstand the significant over-pressured pore-pressure regime. The well was perforated across 40mAH and tested, but despite the significant overpressures no flow was observed. FMI (and other well logs) cover the entire Dinantian carbonate succession of the LTG-01 well. Petrophysical evaluation (Carlson, 2019) showed that the reservoir is very tight with porosities below 2%. Increased porosity intervals exist and do seem to coincide with dolomitic sections. Vuggy porosity across these sections could even be recognized by the FMI data. Total interpreted fractures add up to 915 up to 1.2 fractures per meter with the majority of the fractures consisting out of partially conductive fractures (595) with only a few continuous conductive fractures (31). Fracture density varies considerably throughout the section, but is highest from 4520 – 4680 mAH and close to the base of the Dinantian. Fracturing at the base is most likely related to faulting. No clear cause was identified for the fracture density from 4520 – 4680 mAH, but it is situated below a strong dip change which likely indicates a fault. A third interval could be present from 4710 – 4800mAH, but increasing fracture density is terminates in a wash out resulting in a poor FMI response. Fractures are predominantly high angle, sub-vertical and oriented mainly in the same direction as the present-day maximum horizontal stress (NW-SE) which can be deduced from the drilling induced fractures. There are indications of fractures oriented near to perpendicular to this orientation, but numbers are small. It can therefore be interpreted that the majority of fractures that were oriented NE-SW were either not formed, not interpreted, or were healed due to the maximum horizontal stress orientation. Despite the fact that the well was perforated across a high fracture density interval and the reservoir was found to be seriously over-pressured, the well was not able to flow. This could be the result of poor perforations, not being able to connect to the reservoir or to the fact that the partially continuous fractures were either not permeable enough and/or did not link up to create an effective fracture network. The well did sustain losses and gains during drilling indicating at least a degree of (induced) fracture connectivity.

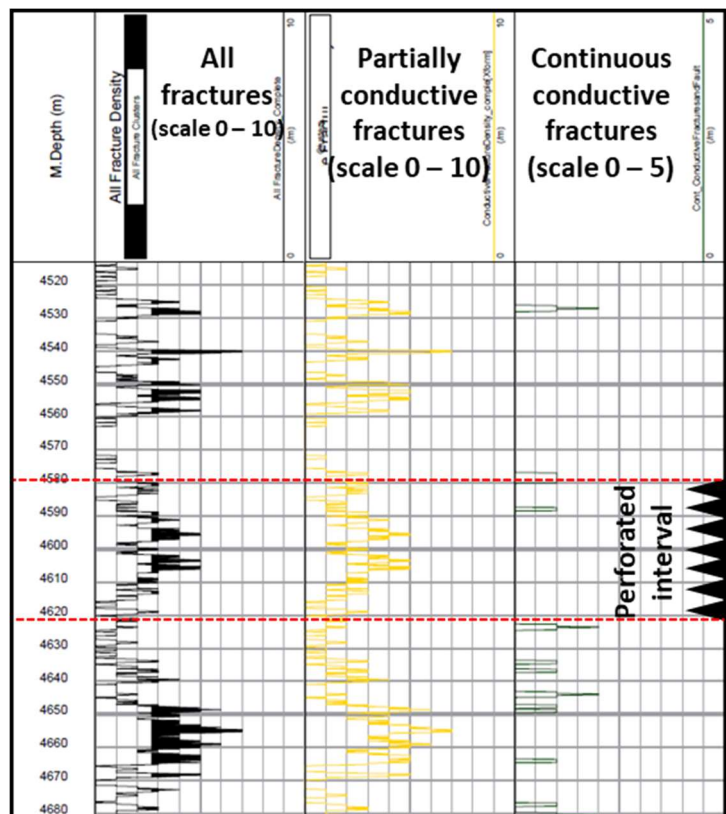


Figure 47: Zoom in on fracture density logs from FMI interpretation across the perforated interval for well testing LTG-01.

The CAL-GT-01 well aimed to prove geothermal development and drilled into larger platform carbonates and carbonate ramp (Mozafari et al., 2019). Today, these carbonates are situated at much shallower depth (~1.6 km) compared to the LTG-01 carbonates (~4.5 km). The Dinantian reservoir was found to be heavily karstified and faulted. The well was drilled without significant overbalance and proved to be productive and was completed as part of a geothermal doublet. Only the top ~150m of the Dinantian was logged by FMI in the CAL-GT-01 well. Petrophysical evaluation (Carlson, 2019) showed that the reservoir is porous although the interpretation is hampered by hole rugosity. From FMI a total of 431 fractures were identified indicating an average fracture density of 3 fractures per meter. Like for LTG-01 the majority consists out of partially conductive fractures (199) and only 10 continuous conductive fractures. Multiple faults were interpreted (13) of which the majority partially conductive (10). Fractures dip pre-dominantly at high angle, sub-vertical and are oriented mainly (WNW-ESE) which is slightly different from the present day active Tegelen fault nearby the well. It seems that these fractures are oriented alike the present day maximum horizontal stress. The well showed good productivity, but due to the karstification and faulting it is difficult to assess to what degree the fracture network contributed to it. It is however likely that the fracturing played an important role in the karstification.

No clear relationships between fracturing and the host rock were derived for the two wells.

7.3 Conclusions FMI

- LTG-01 well sustained losses while drilling, but was drilled overbalanced
- LTG-01 FMI shows that Dinantian carbonate is fractured
- LTG-01 shows large vertical variations in fracture density, average density is ~1.2/m.
- LTG-01 contains 31 continuous conductive fractures out of 915, majority consists out of partially conductive fractures (595)
- LTG-01 fractures are mainly NW-SE oriented
- LTG-01 drilling induced fractures indicated maximum horizontal stress to be NW-SE oriented
- LTG-01 did not produce despite being perforated across interval with high fracture density (partial conductive) and reservoir overpressure. This was apparently a poorly connected and ineffective fracture zone or the fractures were not open
- CAL-GT-01 sustained various drilling issues including heavy losses into a karstified/fractured zone
- CAL-GT-01 faulting, fractures and possible karst causing hole rugosity limited FMI logging
- CAL-GT-01 is heavily fractured resulting in an average fracture density of ~3/m
- CAL-GT-01 only 10 out of 431 fractures are continuous conductive fractures, majority (199) are partially conductive
- CAL-GT-01 fractures are mainly WNW-ESE oriented
- CAL-GT-01 drilling induced fractures are not often observed, but the ones interpreted indicated maximum horizontal (present day) stress to have NW-SE orientation
- Fracture orientation in CAL-GT-01 is different from the major Tegelen fault orientation
- Almost all fractures have a very steep dip (sub-vertical, >70°)
- Fracture density could not be (easily) correlated to other log observations
- MOL-GT FMI interpretation point towards average fracture aperture of 170 microns
- Heibaart DZH1 well core study indicates that there may be a relation between fracture density and facies (mechanical stratigraphy)

8 Conclusions

- For exploration and development purposes it is important to determine where the highest chance of encountering (open) fractures is within the reservoir (both laterally and vertically), and how the (open) fractures are mainly oriented.
- Fracture characteristics are influenced by various factors, like geological and hydrological history, historic and present day stress state, possibly by bed thickness, facies, lithology, mechanical stratigraphy. For these reasons these characteristics vary vertically and laterally within the same rock.
- Finding relationships between fracture characteristics and the factors mentioned above requires insights into the timing of each individual factor and how this influenced the fractures.
- Various data sets can be used (e.g. core, logs, well tests, analogues) which will help to develop an understanding of the fracture characteristics, but all come with limitations including correlatability between data points and extrapolating away from the observations.
- Analysis of Dutch Dinantian fracture characteristics suffers from the large lack of data. This, combined with the varying nature of fracture characteristics, makes correlation between local and regional observations extremely difficult, near impossible.
- Because of the reasons mentioned above, clear relationships between fractures and geological variables are not available for the Dinantian carbonates. Indications for such relations may exist (e.g. DHZ1 (Heibaart) well), but they remain local observations.
- High resolution 3D seismic could provide indirect information on where fracture density may increase. It may provide insights in mechanical variation within the reservoir and therefore variation in fracture characteristics, if the 3D data can be calibrated with sufficient well data.
- BHI data is very useful to identify fracture orientation, open fractures and present day stress state at subsurface conditions. Two FMI data points indicate that conductive (open) fractures are parallel to present day maximum horizontal stress (see also paragraph 7.3).
- The majority of the Dutch Dinantian wells have indications (mostly indirect) that fractures are present and may allow for a degree of flow. However, examples of LTG-01 show complexity of fractured systems as the well was perforated at an interval with increased fractures interpreted, but no flow was achieved despite the significant overpressure.
- Analogue outcrop can be useful for understanding, seeing and measuring fractures, but has limitations to apply quantified variables to subsurface conditions.
- Therefore, flow prediction for fractured Dinantian carbonate reservoir will be very uncertain. Literature and analogues indicate that fracture density is higher near faults and certain parts of folds. Fracture aperture widths varies considerably from only a few, to hundreds of microns. It is estimated that the average for subsurface conditions will be more likely tens of microns than hundreds.
- Well placement decisions are heavily impacted by the expected and observed vertical and horizontal variation in fracture characteristics.

9 Recommendations

- For evaluating pre-drill productivity use wide ranges of scenarios to estimate flow and geothermal power
- For each scenario use a wide range of fracture characteristics
- Try to define 'sweet spots' by creating maps where favorable fracture characteristics may be more likely (faults, folded areas, mechanical stratigraphy, other), but do not step into the pitfall over quantifying statistics as your estimate will likely be based on very limited data
- For exploration and development, focus on fracture density and orientation w.r.t. present day stress.
- Create a strategy for exploration and development well planning & design and how this will result in providing answers to major uncertainties.
- Any new well in the near future targeting the Dinantian carbonates (including non-UDG wells) should accommodate substantial data acquisition across the reservoir section (e.g. borehole imaging, acoustic logs, core).
- Define a solid data acquisition plan pre-drill and also consider this in your well planning strategy. BHI log and well test should be part of the data gathering package.

10 Acknowledgements

The Dutch Ministry of Economic Affairs is thanked for funding this study as part of the SCAN project.

The following people are thanked for their contribution to this study either by providing data, reviewing this document or discussions on fractured carbonates in general: Angela Pascarella, Dominique Reith, Mahtab Mozafari, Henk van Lochem, Bastiaan Jaarsma, Prof. Quinten Fisher, Johan ten Veen, Marieke den Dulk, Jan ter Heeghe, Sander Osinga, Pieter Bruijnen, Ben Dewever, Armelle van Kloppenburg, Eva van der Voet

11 References

- Amantini, E., Ricaud, Y., Grégoire, N., 2009. Development of the performance of the Loenhout UGS (Antwerp-Belgium) – Drilling through a highly karstified and fissured limestone reservoir under gas storage operation. World Gas Conference 2009. Downloadable from; <http://members.igu.org/html/wgc2009/papers/docs/wgcFinal00561.pdf>
- Bai, T., Pollard, D.D., Fracture spacing in layered rocks: a new explanation based on the stress transition. *Journal of Structural Geology* 22, 43-57.
- Bisdom, K., 2016. Burial-related fracturing in sub-horizontal and folded reservoirs: Geometry, geomechanics and impact on permeability. Doctoral Thesis, from: <https://doi.org/10.4233/uuid:f1b6f6e0-1542-4744-943e-04c7c551213b>
- Bisdom, K., Bertotti, G., Nick, H.M., 2016. A geometrically based method for predicting stress-induced fracture aperture and flow in discrete fracture networks, *AAPG Bulletin*, v. 100, no. 7 (July 2016), pp. 1075–1097: DOI:10.1306/02111615127
- Boersma, Q., Prabhakaran, R., Bezerra, F.H. & Bertotti, G., 2019. Linking natural fractures to karst cave development: a case study combining drone imagery, a natural cave network and numerical modelling. *Petroleum Geoscience*
- Bouroullec, R., Nelskamp, S., Kloppenburg, A., Abdul Fattah, R., Foeken, J.P.T., ten Veen, J.H., Geel, C.R., Debacker, T., Smit, J. (2019) Burial and Structural Analysis of the Dinantian Carbonates in the Dutch Subsurface (SCAN). Downloadable from www.nlog.nl
- Boxem, T.A.P., J.G. Veldkamp and J.D.A.M. van Wees: Ultra-diepe geothermie: Overzicht, inzicht & to-do ondergrond, TNO 2016 R10803 (2016)
- Brar N. S. & Stesky R. M., 1980, Permeability of intact and jointed rock. *Eos* 61(46), 1112
- Breislin, C.J., 2018, Basin-Scale Mineral and Fluid Processes at a Platform Margin, Lower Carboniferous, UK https://www.research.manchester.ac.uk/portal/files/77565727/FULL_TEXT.PDF
- Broothaers, M., Bos, S., Lagrou, D., Harcouët-Menou, V., Laenen, B., 2019. Lower Carboniferous limestone reservoir in northern Belgium: structural insights from the Balmatt project in Mol. *Proceedings European Geothermal Congress 2019*. <http://europeangeothermalcongress.eu/wp-content/uploads/2019/07/145.pdf>
- Bruinen, P.M. (2019). Estimating geothermal power of ultra-deep Dinantian carbonates in the Dutch subsurface (SCAN). Downloadable from: www.nlog.nl/scan
- Buijze, L. et al. (2019). Review of worldwide geothermal project mechanisms and occurrence of induced seismicity. Downloadable from: <http://publications.tno.nl/publication/34634288/pWIZ4Q/TNO-2019-R10043.pdf>
- Carlson, T., 2019. Petrophysical Report of the Dinantian Carbonates in the Dutch Subsurface: facies analysis and diagenetic evolution of the Dinantian carbonates in the Dutch subsurface. SCAN Report, April 2019, 26 p. Report downloadable from www.nlog.nl/scan.

- Choi, J.-H., Edwards, P., Ko, K., Kim, Y.-S., 2016. Definition and classification of fault damage zones: A review and a new methodological approach. *Earth-Science Reviews* 152, 70 – 87
- Cosgrove, 2015. The association of folds and fractures and the link between folding, fracturing and fluid flow during the evolution of a fold–thrust belt: a brief review. From: Richards, F. L., Richardson, N. J., Rippington, S. J., Wilson, R.W. & Bond, C. E. (eds) *Industrial Structural Geology: Principles, Techniques and Integration*. Geological Society, London, Special Publications, 421, <http://dx.doi.org/10.1144/SP421.11>
- Davatzes, N.C., and S.H. Hickman, 2010., Stress, fracture, and fluid-flow analysis using acoustic and electrical image logs in hot fractured granites of the Coso geothermal field, California, U.S.A., in M. Pöppelreiter, C. García-Carballido, and M. Kraaijveld, (eds.), *Dipmeter and Borehole Image Log Technology: AAPG Memoir*, v. 92, p. 269-293.
- De Keijzer, M., Hillgartner, H., Al Dhahab, S., Rawnsley, K., 2007. A surface-subsurface study of reservoir-scale fracture heterogeneities in Cretaceous carbonates, North Oman. From: Lonergan, L., Jolly, R.J.H., Rawnsley, K., Sanderson, D.J. (eds) *Fractured Reservoirs*. Geological Society, London, Special Publications, 270, 227-244
- Dennis, P.F., Myhill, D.J., Marca, A., Kirk, R., 2019. Clumped isotope evidence for episodic, rapid flow of fluids in a mineralized fault system in the Peak District, UK. *Journal of the Geological Society*, Vol. 176, pp. 447-461
- Di Cuia, R., Gout, C., Balzagette, L., Masse, P., Vieban, F., 2005. Reservoir Connectivity in a Complex Fractured Reservoir: The Relationship Between Fracturing and Facies in the Upper Cretaceous Apulian Platform of the Maiella Mountain, Southern Italy. Conference: International Petroleum Technology Conference, 2005.
- Freites, A., Geiger, S., and Corbett, P., 2019. Well Test-Derived Permeability in Naturally Fractured Reservoirs with Heterogeneous and Disconnected Fractures. Paper presented at 81st EAGE Conference and Exhibition 2019.
- GEO Education: Fracture, Fracture Everywhere, GEOExPro, Vol. 11 No. 3
https://assets.geoexpro.com/uploads/e6b416b1-e0bd-4f1d-ad22-a8e4365d22c6/GEO_ExPro_v11i3.pdf
- Hakami, E., 1989. Water flow in single rock joints. Technical report Stripa Project, downloadable from: <https://inis.iaea.org/collection/NCLCollectionStore/Public/21/042/21042656.pdf?r=1&r=1>
- Hals, K.M.D., Berre, I., 2012. Thermal Fracturing of Geothermal Wells and the Effects of Borehole Orientation. Submitted December 2012. [arXiv:1212.2763](https://arxiv.org/abs/1212.2763)
- Hance, L., Poty, E., DeVuyst, F.-X., 2006a. Tournaisian, *Geologica Belgica*, 9/1-2: 47-53
- Hance, L., Poty, E., DeVuyst, F.-X., 2006b. Viséan, *Geologica Belgica*, 9/1-2: 55-62
- Hardebol, N. J., C. Maier, H. Nick, S. Geiger, G. Bertotti, and H. Boro (2015), Multiscale fracture network characterization and impact on flow: A case study on the Latemar carbonate platform, *J. Geophys. Res. Solid Earth*, 120, 8197–8222, doi:10.1002/2015JB011879.
- Hornby, B. E., Johnson, D. L., Winkler, K. W. & Plumb, R. A. 1989. Fracture evaluation using reflected Stoneley wave arrivals. *Geophysics*, 54, 1274-1288.

- Huang, J., Griffiths D.V., Wong, S.W., 2011. Characterizing Natural-Fracture Permeability From Mud-Loss Data. SPE Journal, March, 111-114.
- Jamison, W., Rait, G, and Dunn, L., 2007. Fracture System Characteristics in Folded Mississippian Carbonates: Livingstone River Anticline at Beaver Creek. Paper presented at the “Let it Flow – 2007 CSPG CSEG Convention”, p.229-230
- Klimchouck, A., Auler, A.S., Bezerra, F.H.R., Cazarin, C.L., Balsamo, F. & Dublyansky, Y. 2016. Hypogenic origin, geologic controls and functional organization of a giant cave system in Precambrian carbonates, Brazil. *Geomorphology*, 253, p. 385-405
- Laubach, S.E., 2003. Practical approaches to identifying sealed and open fractures AAPG Bulletin, v. 87, no. 4, pp. 561–579
- Laubach, S.E, Lander, R., Criscenti, L., Anovitz, L.M., Urai, J., Pollyea, R., Hooker, J., Narr, W., Evans, M.A., Kerisit, S.N., Olson, J., Dewers, T., Fisher, D., Bodnar, R., Evans, B., Dove, P., Bonnell, L.M., Marder, M.P., Pyrak-Nolte, L., 2019. The Role of Chemistry in Fracture Pattern Development and Opportunities to Advance Interpretations of Geological Materials. *Reviews of Geophysics*, DOI: 10.1029/2019RG000671
- Lietard, O., Unwin, T., Guillot, D., Hodder, M.H., 1999. Fracture Width Logging While Drilling and Drilling Mud/Loss-Circulation-Material Selection Guidelines in Naturally Fractured Reservoirs. *SPE Drill & Compl* 14 (3), 168-177.
- Lietard, O., Unwin, T., Guillot, D., Hodder, M.H., (2002) Fracture Width Logging While Drilling and Drilling Mud/Loss-Circulation-Material Selection Guidelines in Naturally Fractured Reservoirs. *SPE Drill & Compl* 17 (4), 237-246
- Luthi, S. M. & Souhaité P. 1990. Fracture apertures from electrical hole scans: *Geophysics*, 55, 821-833.
- Mozafari, M., Gutteridge, P., Riva, A., Geel, C. R., Garland, J., and Dewit, J. (2019). Facies analysis and diagenetic evolution of the Dinantian carbonates in the Dutch subsurface (SCAN). Downloadable from www.nlog.nl
- Nelson, R.A., 2001. *Geologic Analysis of Naturally Fractured Reservoirs*. 2nd edition, *Gulf Professional Publishing an imprint of Butterworth-Heinemann*, ISBN 0-88415-317-7
- Osinga, S. and Buik, N., 2019. Stress field characterization in the Dutch Dinantian Carbonates. SCAN Report, SCAN Dinantien – 2.4 Stress Field, 2019. Report downloadable from www.nlog.nl/scan
- Peacock, D.C.P., Harris, S.D., Mauldon, M., 2003. Use of curved scanlines and boreholes to predict fracture frequencies. *Journal of structural geology* 25, 109 – 119
- Petitclerc, E., Welkenhuysen, K., Van Passel, S., Piessens, K., Maes, D., Compernelle, T., 2017. Development of the first deep geothermal doublet in the Campine Basin of Belgium. *European Geologist Journal* 43. Link: <https://eurogeologists.eu/european-geologist-journal-43-bos-development-of-the-first-deep-geothermal-doublet-in-the-campine-basin-of-belgium/>

- Poty, E., 2016. The Dinantian (Mississippian) succession of southern Belgium and surrounding areas: stratigraphy improvement and inferred climate reconstruction. *Geologica Belgica*, 19/1-2: 177-200
- Reijmer, J., Ten Veen, J., Jaarsma, B., & Boots, R., 2017. Seismic stratigraphy of Dinantian carbonates in the southern Netherlands and northern Belgium. *Netherlands Journal of Geosciences*, 96(4), 353-379. doi:10.1017/njg.2017.33
- Reith, D., 2018. Dynamic simulation of a geothermal reservoir, Case study of the Dinantian carbonates in the Californië geothermal wells, Limburg, NL. MSc thesis TU Delft. <https://kennisbank.ebn.nl/wp-content/uploads/2019/05/Msc-thesis-Dominique-Reith-TU-Delft.pdf>
- Richard, P., Pattnaik, C., Al Ajmi, N., Kidambi, V., Narhari, R., 2015. Discrete Fracture Network models in Support of Drilling Activities in North Kuwait Carbonate Reservoirs. SPE Kuwait Oil & Gas Show and Conference held in Mishref, Kuwait. SPE-175375-MS
- Rolando, J.P., Massonat, G.J., Grasso, J.R., Odonne, F., and Meftahi, R., 1997. Characterization and modelling of increasing permeability while producing a gas fractured reservoir. SPE paper 38711, presented at the 1997 SPE annual Technical Conference and Exhibition held in San Antonio, Texas, 5-8- October 1997.
- Sibbit, A. M. & Faivre, O., 1985. The Dual Laterolog Response in Fractured Rocks. Paper T, presented at the 26th Annual Logging Symposium of the SPWLA (Dallas, TX).
- Ten Veen, J.H., de Haan, H.B., de Bruin, G., Holleman, N., Schöler, W. (2019). Seismic Interpretation and Depth Conversion of the Dinantian carbonates in the Dutch subsurface (SCAN). Downloadable from www.nlog.nl/scan
- Ter Heege, J.H., Osinga, S. and Carpentier, S., 2018. The geomechanical response of naturally fractured carbonate reservoirs to operation of a geothermal doublet, *ARMA* 18 – 791
- Van der Voet, E., Muchez, P., Laenen, B., Weltje, G.J., Lagrou, D., Swennen, R., *In press*, Characterizing carbonate reservoir fracturing from borehole data – A case study of the Viséan in northern Belgium. *Marine and Petroleum Geology*, Volume 111, Pages 375 – 389, <https://www.sciencedirect.com/science/article/pii/S026481721930412X?via%3Dihub>
- Van Golf-Racht, T. D., (1982), *Fundamentals of Fractured Reservoir Engineering*. Elsevier Publishing Company, 710 pp.
- Veldkamp, J.G., Loeve, D., Peters, E., Nair, R., Pizzocolo, F., Wilschut, F., 2016. Thermal fracturing due to low injection temperatures in geothermal doublets. Downloadable from <https://www.nlog.nl/rapporten>
- Walsh, J.B., 1981. Effect of Pore Pressure and Confining Pressure on Fracture Permeability. *Int. J. Rock Mech. Min. Sci. & Geomech. Abstr.* Vol. 18, pp. 429 to 435.
- Zimmerman R, Main I, 2004. Chapter 7 - Hydromechanical Behavior of Fractured Rocks. In: *Mechanics of Fluid-Saturated Rocks* (ed. By Yves Guéguen, Maurice Boutéca) Volume 89, Pages: 363-421.

Zoback, M. and Moos, D., 1988. In-situ stress, natural fracture and sonic velocity measurements in the Moodus, CT Scientific Research Well. In: Woodward-Clyde Consultants, Moodus, CT Borehole Research Project: The magnitude and orientation of tectonic stress in southern New England. Final Report EP86-42 to the Empire State Electric Energy Research Corp., Northeast Utilities, and Electric Power Research Institute. New York, Appendix C.

12 Appendix A: Data table well data

Table 7: Available data for the Dutch wells drilled in the Dinantian carbonates (from Mozafari et al, 2019)

Well name	Well tops	Wireline logs	Biostrat	Litholog	Core Total length (m)	New core description	CCAL	Core thin sections	Cuttings TS	C and O Isotopes	S Isotopes	FI	VR	Purpose	Year of drilling
BHG-01	X	X	X*	X	25.8	X	X	74+6*	-	9*	3*	2	10+2*	HC- exploration	1978
CAL-GT-01	X	X	-	-	-	-	-	-	X	-	-	-	-	Geothermal energy	2012
CAL-GT-02	X	X	-	-	-	-	-	-	12	-	-	-	-	Geothermal energy	2012
CAL-GT-03	X	X	-	-	-	-	-	-	-	-	-	-	-	Geothermal energy	2012
DB-105	X	-	-	-	-	-	-	-	-	-	-	-	-	Exploration	1920
DB-106	X	-	-	-	-	-	-	-	-	-	-	-	-	Exploration	1920-1921
DB-109 Cadier en Keer	X	-	X	X	N.A	-	-	-	-	-	-	-	-	Exploration	1920-1921
DB-108 MESCH	X	-	X	-	N.A	-	-	-	-	-	-	-	-	Exploration	1922
DB-123 Kastanjelaan	X	-	X	-	N.A	-	-	-	-	-	-	-	-	Exploration	1927-1929
GVK-01	X	X	X	X	695	-	X+SCAL	-	-	2	-	1	31	Exploration	1986
HEU-01	X	X	-	-	188	X	X	70	-	-	-	-	-	Mineral water	1981
HEU-01-S1	X	X	-	-	193	X	X	33	-	-	-	-	13	Mineral water	1981
KSL-02	X	X	-	-	164.05	X	X	43+5*	-	7*	-	1*	5	Mineral water	1981
KTG-01	X	X	X*	X	51	X	X	69+5*	-	18*	-	2*	-	HC- exploration	1982
LTG-01	X	X	X	-	5.5	X	X	9	16	-	-	-	-	HC- exploration	2004-2005
O18-01	X	X	X	X	53.46	X	X	23+2*	1	37+4*	-	2+1*	13	HC- exploration	1991
P16-01	X	-	X	X	-	-	-	-	-	-	-	-	18	HC- exploration	1991
S02-02	X	X	X	-	16	X	-	18	-	-	-	-	22	HC- exploration	1983
S05-01	X	X	X	-	127	X	X	228+4*	-	14*	-	-	5	HC- exploration	1981
THERMAE – 2000	X	-	-	-	-	-	-	-	N.A.	-	-	-	7	Mineral water	1985-1986
THERMAE – 2001	X	-	-	-	-	-	-	-	-	-	-	-	-	Mineral water	1985-1986
THERMAE – 2002	X	(X)	-	-	-	-	-	-	N.A.	-	-	-	9	Mineral water	1985-1986
UHM-02	X	X	X*	-	7	X	X	19	198	12	-	1	1*	HC- exploration	2001
WDR-01	X	-	X	X	N.A.	-	-	-	-	-	-	-	-	HC/coal- exploration?	1912-1914
WSK-01	X	X	X	X	7.4	X	X	11	-	-	-	-	5	HC- exploration	1977-1978

13 Appendix B: Table with fracture indications from drilling, logs, core recovery and well tests

Table 8: Summary of wells with core and or new petrophysical evaluation (Carlson, 2019). Content based on drilling reports, petrophysical reports (Carlson, 2019) and well test reports.

Well Name	Drilling observations	Petrophysical report Carlson (2019)	Core Recovery	Well test
BHG-01	no issues reported for Dinantian section	2413.7m: wash out which is probably caused by a fracture or possibly a karst	Dinantian 2168-2183 m (100 % recovery) 2375-2387 m (100 % recovery) Devonian 2649-2658 m (0 % recovery) 2672-2681 m (100 % recovery) 2901.2-2906 m (100 % recovery)	DST: 1/6/1978: 2406.7-2418.3 m (40 shots), 1. Acid: 5 m3 HCl (28%) (p=250 bar) 2. Coiled tubing + N2 lift : no HC, 18,5 m3 water. Fluid level at 78m after production >> Back prod: 320 L sea water DST: 6/6/1978: 2165-2185 m (68 shots), 1. Acid: 5 m3 HCl (28%) (p=130 bar) : 3,9 m3 sea water + 3,5 m3 acid + H2S (60-80 ppm) 2. Coiled tubing: 4,5 m3 formation water + increasing H2S 3. N2 lift: 15 m3 formation water
CAL-GT-01(-S1)	@1736mMD total losses, drastic increase in ROP, steering issues. @1887mAH check trip, unplanned sidetrack when washing down from loss zone. Continued in new hole. @2082mAH, check trip, returning in hole difficulties in loss zone, hole could not be found. 7"liner run to bottom loss zone 1802mAH. @2345mAH losses 14-20 m3/hr	The 8 ½" hole interval below 1728,5 m has cavernous porosity		Production test: 6-8-2012 / 7-8-2012: Open hole interval (1802 - 2730 m mD) Multi rate step test, ESP frequency increase 5 Hz every 3 hrs. No build-up. Decreasing PI for increasing ESP freq.
CAL-GT-02	Losses after when TD was reached (@1694.3mAH) and BHA was POOH to surface. Irregular ROP's (possibly also related to assembly choices)			Injection test: 20-9-2012 Open hole interval (1402 - 1694 m mD) Multi rate step test, injection pressure increase (approx. 10 bar) every 55/60 min. No fall-off. Decreasing PI for increasing injection pressure.

Well Name	Drilling observations	Petrophysical report Carlson (2019)	Core Recovery	Well test
CAL-GT-03	@1622mAH, losses cured with cement plug @2835, losses (fault was expected) @2955,9mAH, increase in torque, increase in losses (up to 60m3/hr)			
CAL-GT-04	not public			
CAL-GT-05	not public			
DB-105	No clear reports			
DB-106	No clear reports			
DB-109 Cadieren Keer	No clear reports			
DB-108 MESCH	No clear reports			
DB-123 Kastanjelaan	No clear reports			
GVK-01	No clear reports			No test data is available and no wireline formation tester was run in this well. It is likely that this well would produce, both through matrix and through fractures.
HEU-01-S1	No clear reports			
KSL-02	No clear reports			

Well Name	Drilling observations	Petrophysical report Carlson (2019)	Core Recovery	Well test
KTG-01	<p>@964-973mAH losses while coring, 1m³/hr, cured by reducing MW to 1.12 s.g. @964mAH large open frac mentioned in drilling report (probably from core). @972-978 coring stopped due to increasing losses, 5m³ in 8 hrs @978mAH cemented fractures reported. @989 - 996mAH, +/- 7m³ losses while coring</p> <p>Many losses (Cum. 143 m³) reported while drilling Devonian</p>		<p>The core shows a karsted interval (959-962 m, 100% recovered) and is very heterogenous. Other karsted intervals are present in the interval 971.5-983.5 (100% recovery). Kerns 989 - 996mAH (100%)</p>	<p>Open hole DST: 13-10-1982 / 14-10-1982: 930-1051 m (Dinantian)1. Flow to surface (approx. 400 L of liquid)</p> <p>2. Acid: 14,5 m³ HCl (15%) + N₂ lift (1.5 hrs): 369 m³ formation water 3. After the lift: q= 5,4 m³/hr (content: Chlorine 36.6 gr/L + H₂S 50ppm) 4. After close-in: p=2.5 bar at surface</p> <p>RFT 10-10-1982 930-1051 m (Dinantian) 1. RFT test throughout open hole section (9/16 are in Dinantian) 2. All tests > dry test (no permeability) 3. 3 tests (deeper than Dinantian) have seal failure > due to enlarged borehole (for ex. Due to fractures)</p>

Well Name	Drilling observations	Petrophysical report Carlson (2019)	Core Recovery	Well test
LTG-01	<p>In this well the invasion/losses are severe, and the resistivity is affected severely by this. Minor losses were recorded from @4450 mAH, minor losses (cum 400L) @4585 - 4600m AH, losses 4m3/hr @4606 mAH, losses (cum total 48m3) Wiper trip, circulation, losses 114m3. Circulation for 2nd MDT, 60m3 losses. Reaming, losses 5m3/hr, 22m3 total. Drilled on with dynamic losses 2m3/hr up to 25m3/hr. @4847 to 4925 mAH, minor gains were detected. @5023 m AH (near top Devonian): Minor to major losses at <148 l/min to >15 m3/hr. Mud density 1460 - 1470 kg/m3. @4776 - 4835mAH, losses, FMI got stuck (The gains may be an indication of so called ballooning where the mud is first lost into the formation in fractures or porous sections and then, when the hydrostatic head is slightly lower, due to small variations in mud density, the fluids initially lost to the formation flows back into the wellbore. This is not an uncommon feature in carbonate rocks.)</p>	<p>The poor hole conditions in some intervals, particularly 4775-4798 m. In the three upper thicker intervals (4474-4500 m, 4572-4597 m, 4760-4795 m) the porosity is very erratic pointing to karstic nature of the porosity development. One very anomalous interval is between 4765-4769 m ... the possibility of the neutron seeing a reasonable sized void away from the actual borehole. Between 4830 and 4980 m there are a significant number of lower resistivity spikes ... Fractures could be one explanation ... but cannot be confirmed.</p>	<p>4376-4379.5 m (2.4 m recovered, 69 %) 4470-4480 m (3 m recovered, 30 %).</p>	<p>Production test 8/3/2005 (?) 4580-4620 m 1. No flow recorded at surface for BHP = 407 bar at 4475m 2. No record of acid stimulation 3. No test report</p> <p>DMT 11-9-2004 29-9-2004 3-10-2004 4604-4605 m 1. Result: Dinantian is overpressured (approx. 140 bar, minimum overpressure value is 69 bar with salt saturated water density 1190 kg/m3) 2. Porous intervals are poorly connected (supercharge pressures measured in few pressure points) 3. Porous interval around 4604.5m is possibly connected to larger system</p>

Well Name	Drilling observations	Petrophysical report Carlson (2019)	Core Recovery	Well test
O18-01	Wash outs experienced while drilling towards 7122 ftAH @7122 ftAH, drilling break, total loss circulation. stabilised at 9.1-9.2 ppg.	... numerous washouts ... The highest porosity interval is 2170-2180 m where the porosity exceeds 2 % over 10 m with the highest porosity, 11.5 %, at the top of the interval. This interval has some very sharp break outs and it is quite possible that this is caused by fractures. The erratic behavior of the logs is indicative of karsting possibly associated with fractures. Below this interval down to 2220 m there are several more very thin porosity spikes.	Core 1: 1181.4-1199.7 m (Westphalian) (100 % recovery) Core 2: 1199.7-1218 m (Westphalian) (97 % recovery) Core 3: 1600.2-1610.9 m (Dinantian) (100 % recovery) Core 4: 1610.9-1614.8 m (Dinantian) (100 % recovery) Core 5: 2064.7-2076.1 m (Dinantian) (100 % recovery) Core 6: 2612.4-2639.9 m (Dinantian) (100 % recovery) Core 7: 3034.3-3051.4 m (Devonian) (100 % recovery)	Open hole DST: 1602-2862 m 1. N2 lift: no flow to surface, minor inflow downhole 2. lowest downhole pressure after N2 lift = 133 bar 3. no acid stimulation FMT 11-5-1991 1179-2179 m (17 points) 1. No inflow, all dry tests / seal failures
P16-01	only 13m drilled into Dinantian			

Well Name	Drilling observations	Petrophysical report Carlson (2019)	Core Recovery	Well test
S02-02	<p>There were no losses recorded in the Dinantian section. Overbalance is approximately 35-40 bar, quite considerable and it is likely that losses would occur if there were open fractures and/or open karst.</p>	<p>.. many wash outs ...</p> <p>at 1883 m down to approx. 2730 m. In this interval, there are porosity spikes at 1889.5 m and 1895.5 m, close to the top of the reservoir. These two short porosity spikes could be karst infilled with some clay,</p> <p>The following porosity spikes are at 2100 m and at 2110 m, with very pronounced anomalies on sonic, density and resistivity, although the use of the porosity from the resistivity limits the second one, such that only the first exceeds 2 %. These could be fractures or very limited karst. In the interval 2203-2226 m, there are 6 very short intervals (<1 m thick) with porosity exceeding 2 % (3-5 %). These are probably karsts.</p> <p>The best porosity interval is 2780-2812 m with some porosities as high as 4-7 %, this is also part of the most dolomitic section of the well. The rapid variation in porosity points to that this is a karsted section.</p>	<p>1886-1889 m, recovery 1.8 m (60 %); 1889-1898 m, recovery 5.5 m (61 %); 2417.3-2426.3 m, recovery 0.9 m (10 %), mostly rubble; 2615.8-2624.9, recovery 1.5 m (16 %); 2624.9-2633.4 m, recovered 5.9 m (70 %).</p>	<p>FMT 17-11-1983 (18 points) / 18-11-1983 (6 points) 1870-2791 m</p> <p>1. 2 points on run 1 were stable (1 above top Dinantian, 1 in Dinantian): pressure point in Dinantian slightly supercharged (2.5 bar when comparing pressure gradient from pressure points above)</p> <p>2. 2 points on run 2 were stable (both above top dinantian)</p>

Well Name	Drilling observations	Petrophysical report Carlson (2019)	Core Recovery	Well test
S05-01	<p>@1240 - 1800 mAH, large losses of 664 m3</p> <p>@1317mAH losses up to 4m3/hr, 4 10m3 LCM pills, losses in total 65m3</p> <p>@ 1360 mAH, losses, LCM, cumm losses 94 m3</p> <p>@ 1410mAH losses up to 1.5 m3/hr, cumm losses 108m3</p>	<p>The interval 1439-1448 m is the only thicker, more porous, interval in the upper part of the Dinantian. It has several small sharp wash-outs, indicating that it could be fractured and at the base, a distinct small clay layer according to the spectral GR. It is therefore likely that it is a karsted interval with some clay infill and fractures.</p> <p>The best porosity (2-6 % porosity) interval 1968-1987 m is Dolomite ...</p> <p>Only one very small perturbation on the caliper could indicate fracturing. The porosity is related to secondary processes and it is relatively likely that karsting has played a role.</p>	<p>1190-1199 m (recovered 1190-1192 m, 22 %, but also reported no progress, recovery could be operational), 1199-1210 m (recovered 100 %), 1210-1228 m (recovered 100 %), 1228-1240 m (100 % recovery), 1349-1360 m (100 % recovery), 1668-1682 m (100 % recovery), 1784-1802 m (100 % recovery), 1904-1906 m (100 % recovery), 1906-1913 m (100 % recovery), 2015-2029 m (100 % recovery), 2130-2148 m (100 % recovery).</p>	<p>RFT 4-7-1981</p> <p>1230-1990 m (35 points)</p> <p>1. 1 pressure test showed flow (depth 1481,2 m, in Dinantian), the rest mostly dry test and some seal failures</p> <p>2. Dinantian might be slightly overpressured, not possible to determine with 1 pressure point</p> <p>DST 13-7-1981</p> <p>Perforations: 1911-1943 (108 shots total)1. Acid: 30 m3 (max inj pressure 157 bar) + N2 lift : 47,4 m3 produced water, no H2S</p> <p>DST 18-7-1981</p> <p>Perforations: 1480-1491 & 1430-1451 (107 shots total)1. Acid: volume not provided (max inj pressure 330 bar) + N2 lift : 70,7 m3 liquid + no H2S</p> <p>DST 19-7-1981</p> <p>Perforations: 1189-1200 & 1225-1236 (74 shots total)1. Acid: 22 m3 + N2 lift : 245 m3 liquid + no H2S</p>
THERMAE - 2000	No clear reports			
THERMAE - 2002	No clear reports			

Well Name	Drilling observations	Petrophysical report Carlson (2019)	Core Recovery	Well test
UHM-02	@4751 mAH, losses @5123 – 5170mAH, losses @5238m, heaviest losses initial rate of 10m3/hr.	<p>A strange feature is that there are some long intervals with surprisingly low resistivity, although the porosity is very low. The first such interval is 4836-5007 m, the second 5119-5144, the third 5264-5333 m. The low resistivity is associated with elevated Uranium content and in some places with many Uranium spikes. This could indicate fractures and another possibility is dispersed conductive minerals, something that has a prominent influence on induction tools.</p> <p>At 5165 m there is a very high porosity interval, up to 30 %, with very low resistivity and at 5250 m there is thicker high porosity interval.</p> <p>This would then most likely be explained by a karsted interval or an interval with large to very large vugs. However, it cannot be excluded that the high PEF is caused by Baryte in the actual rock,</p>	4751-4758 m was cored with a core recovery of 98 %.	<p>RFT 8-4-2002 4699,7-4826 m (21 points) 1. All tests are dry + seal failures</p> <p>MDT 10-5-2002 5145.5 m 1. One pressure point in dinantian: 706,9 bar at 5141,9 m TVDss 2. Overpressure is 103-178 bar depending on density of fluid used 3. Fluid sample of formation water: salt saturated brine with large content of metals (zink+lead+Cadmium + Barium)</p>
WDR-01	Only 29m drilled Dinantian			

Well Name	Drilling observations	Petrophysical report Carlson (2019)	Core Recovery	Well test
WSK-01	No issues (losses, gains) reported		First coring session, BHA got stuck, jarred free. 4232-4241 (100 % recovery) Second coring session, BHA got stuck, BHA released, fished, jarred and recovered. 4433-4441.5 m (100 % recovery)	Production test 7-2-1978 Perforations: 4299-4322 (301 shots) 1. Acid: 16,8 m3 (10%) (MSA): no inflow 2. Unlikely that Dinantian is overpressured, based on mud density (no pressure points)

14 Appendix C: Table of data files shared via www.nlog.nl/scan

Table 9: List of FMI interpretation files shared via www.nlog.nl/scan

Well	Content	File name	Format
LTG-01	Interpretation panel	SCAN Fracture Characterisation Dinantian - results LTG-01_FMI interpretation_SCALE_100	pdf
LTG-01	Interpretation panel	SCAN Fracture Characterisation Dinantian - results LTG-01_FMI int panel SCALE_1000	pdf
LTG-01	Interpretation data bedding	SCAN Fracture Characterisation Dinantian - results LTG-01_FMI_bedding	txt
LTG-01	Interpretation data drilling induced fractures	SCAN Fracture Characterisation Dinantian - results LTG-01_FMI_drilling_induced_features	txt
LTG-01	Interpretation data fracture density curve	SCAN Fracture Characterisation Dinantian - results LTG-01_FMI_FractureDensity	LAS
LTG-01	Interpretation data fractures	SCAN Fracture Characterisation Dinantian - results LTG-01_FMI_fractures	txt
LTG-01	Interpretation data textural observations	SCAN Fracture Characterisation Dinantian - results LTG-01_FMI_textural_observations	txt
CAL-GT-01	Interpretation data bedding	SCAN Fracture Characterisation Dinantian - results CAL-GT-01 FMI bedding	txt
CAL-GT-01	Interpretation data drilling induced fractures	SCAN Fracture Characterisation Dinantian - results CAL-GT-01 FMI drilling induced features	txt
CAL-GT-01	Interpretation data fractures	SCAN Fracture Characterisation Dinantian - results CAL-GT-01 FMI fractures	txt
CAL-GT-01	Interpretation panel	SCAN Fracture Characterisation Dinantian - results CAL-GT-01_FMI int panel_SCALE_100	pdf
CAL-GT-01	Interpretation panel	SCAN Fracture Characterisation Dinantian - results CAL-GT-01_FMI int panel_SCALE_1000	pdf
CAL-GT-01	Interpretation panel	SCAN Fracture Characterisation Dinantian - results CAL-GT-01_FMI int panel_SCALE_500	pdf
CAL-GT-01	Interpretation data fracture density curve	SCAN Fracture Characterisation Dinantian - results CAL-GT-01_FMI_Fracture Density	LAS

Onderzoek in de ondergrond voor aardwarmte